Alferyeva Ya.O., Novikova A.S., Gramenitskiy E.N. Interaction of fluorine-containing granite melt and calcite as a possible cause of formation of high-calcium ongonites. UDC 552.113

Lomonosov Moscow State University, Department of Geology, Moscow (YanaAlf@ya.ru)

Abstract. The interaction parameters of high fluoride granite melt and calcite were studied at 750 ° C and pressure of 1 kbar. In the contact area, the redistribution of components and the formation of new minerals are well manifested. A small contribution of calcium to the silicate melt is accompanied by a significant removal of fluorine from it.

Keywords: ongonite, high-fluoride granite.

Ongonites with a high calcium content are described as one of the rock varieties of the Ary-Bulak massif (Eastern Transbaikalia) [Peretyazhko et al., 2007, 2010; Antipin et al., 2009]. Ongonites are formed as a result of crystallization of a highly evolved granite melt rich in fluorine [Kovalenko et al., 1971, 1976, 1979]. In the course of crystallization differentiation, Ca does not accumulate in the residual melt, but is spent on the formation of rock-forming minerals. In magmatic processes, the mechanism of joint accumulation of Ca and F is unknown. It is possible that the high calcium content in the ongonites rich in fluorine is the result of the interaction of the ongonite melt with the host carbonate rocks (Antipin et al., 2009).

The experiment is aimed at studying the parameters of interaction of high-fluorine granite melt and calcite at 750 ° C and a pressure of 1 kbar.

The experiments were carried out at the Institute of Experimental Mineralogy, IEM RAS (Chernogolovka) on a high gas pressure unit UVD10000. LiF, NaF, K_2SiF_6, AlF_3, Al_2O_3, SiO_2 (gel), $NaAlSi_3O_8$, $KAlSi_3O_8$ were used as starting reagents. A charge was made from them, which in terms of the content of Si, Al, Na, K, Li and F is equivalent to low-calcium ongonites of the Ary-Bulak massif (SiO_2 - 72.6, Al_2O_3 - 17.0, Na_2O - 3.9, K_2O - 4.5 , Li_2O - 0.1, F - 1.8 wt%). The platinum ampoule was filled to the middle with this mixture, the second half of the ampoule was filled with crushed calcite. Water was added to the ampoule in an amount of 10% of the weight of the entire sample. The ampoule was welded on both sides. The experiment lasted 5 days.

The results of the experiment showed that between the ongonite melt and carbonate, a contact interaction is established with the formation of zoning (Fig. 1). At the border, a zone is mainly composed of anorthite. Along the contact in the silicate part of the sample, a zone composed of silicate melt and alkaline feldspar. When moving away from the contact, the feldspar disappears. The carbonate part consists of calcite, quartz, wollastonite, cuspidine and a phase, the composition of which varies within wide limits (in at.%): Si - 15-19, Ca - 14-15, F - 16-23, measured O - 45- 51, Na - 0.3, Al and K < 0.1.

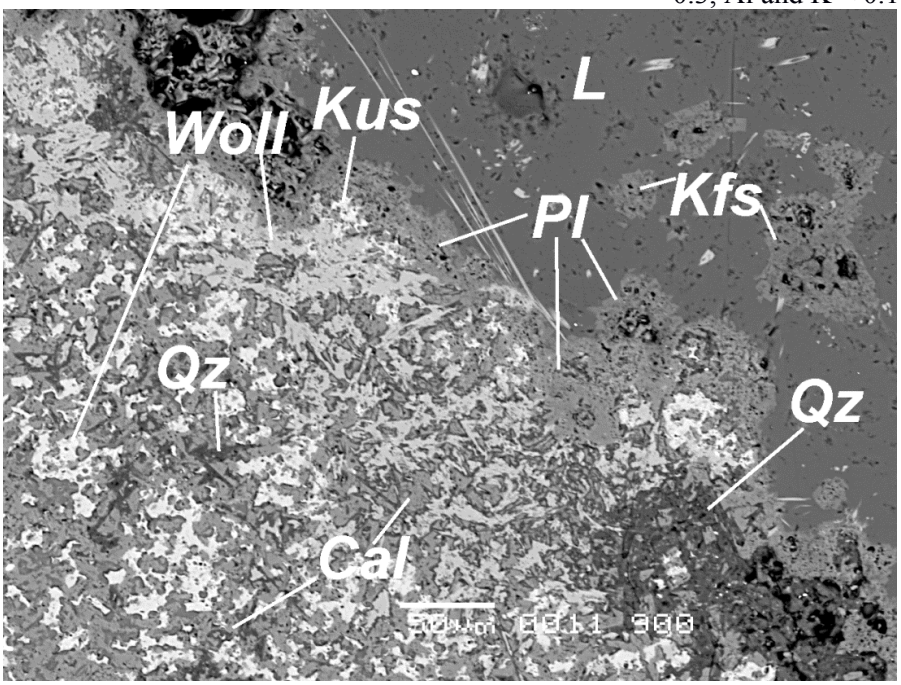

Fig. 1. The contact area of the sample. L - silicate glass, Kfs - alkali feldspar, Qz - quartz, Pl - plagioclase, Woll - wollastonite, Kus - cuspidin, Cal - calcite.

Figure 2 shows the results of measurements of the sample composition over an square area with side length from 100 to 500 μm at different distances from the contact. The carbonate part of the sample over the entire measurement area contains significant

amounts of silica (up to 30 wt%) and fluorine (up to 8 wt%). When approaching the contact, the amount of silica increases, calcium decreases, and the fluorine content has a maximum at a distance of about 1 mm from the contact.When approaching the contact from the side of the silicate part, the fluorine content drops to almost zero, the amount of calcium increases by tenths of a percent. The amount of silicon and aluminum changes only slightly. The contact has a maximum aluminum content.

Conclusion. At the contact of the fluorine-containing granite melt and calcite, there is a well-manifested contact interaction with the redistribution of components and the formation of new minerals. A small redistribution of calcium to the silicate melt is accompanied by a significant removal of fluorine from it. In the experiments carried out, a high-calcium rock with a high fluorine content is formed only in place of a carbonate material.

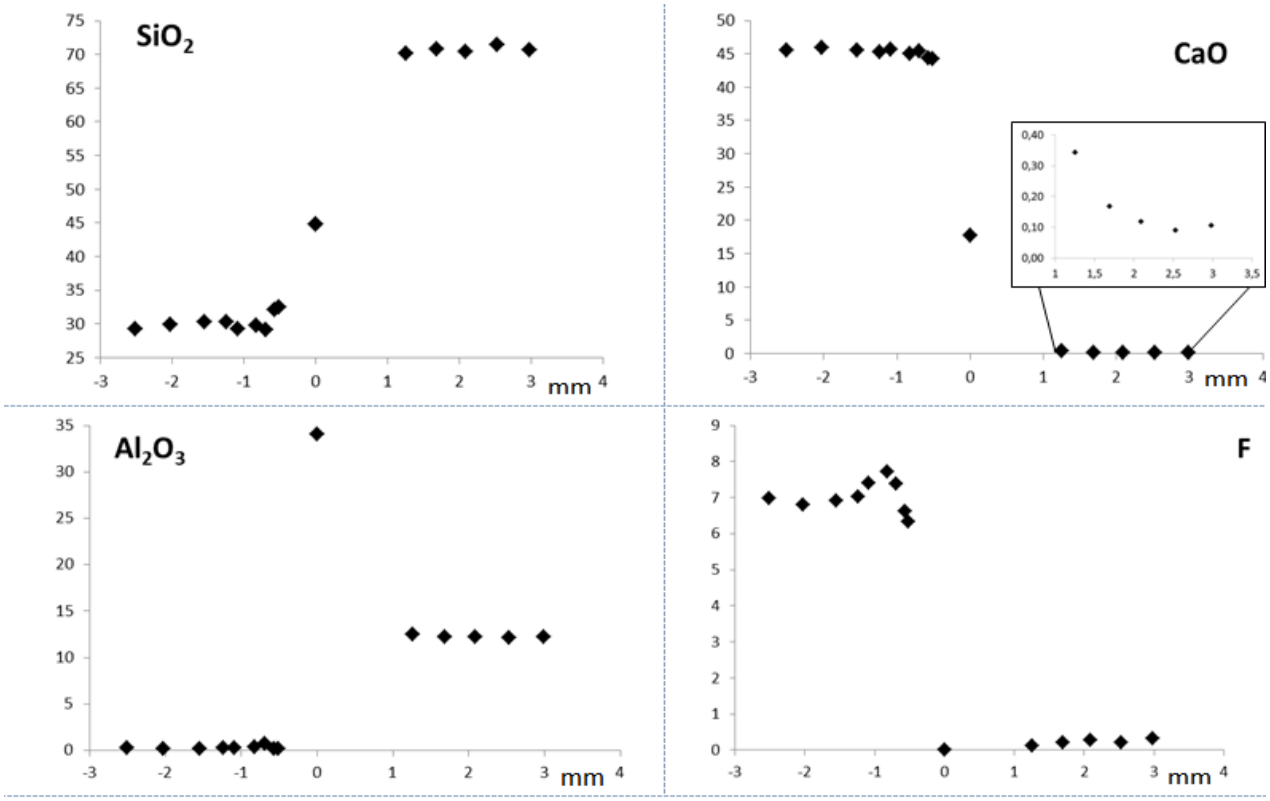

Fig. 2. Content of components in the sample at different distances from the contact. The composition of plagioclase from the contact zone is taken as zero. Positive values on the X axis correspond to the silicate part of the sample, negative values correspond to the carbonate part.

References

Antipin V.S., Andreeva I.A. Kovalenko V.I. Kuznetsov. V.A. Geochemical specifics of ongonites in the Ary-Bulak massif, Easten Transbaikalia // Petrology, vol. 17. 2009. No. 6. P. 558-569.

Kovalenko V.I., Kuzmin M.I., Antipov V.S., Petrov L.L. Topaz-containing quartz keratophyr (ongonite) is a new variety of subvolcanic vein igneous rocks // Reports of the Academy of Sciences of the USSR. 1971. T. 199, No. 2. P. 430-433. In Russian.

Kovalenko V.I., Kovalenko N.I. Ongonites are subvolcanic analogs of rare metal lithium fluoride granites. M.: Nauka, 1976.125 p. In Russian.

Kovalenko N.I. Experimental study of the formation of rare-metal lithium-fluoride granites. M., Nauka, 1979, 85 p. In Russian.

Peretyazhko I.S., Zagorskiy V.E., Tsareva E.A., Sapozhnikov A.N. Immiscibility of fluoride - calcium and aluminosilicate melts in ongonites of the Ary-Bulak massif (Eastern Transbaikalia) // Dokl. RAS, 2007, vol. 413, no. 2, p. 244-250. In Russian.

Peretyazhko I.S., Savina E.A. Fluid and magmatic processes in the formation of the Ary-Bulak ongonite massif (Eastern Transbaikalia) // Geology and Geophysics. 2010.Vol. 51, pp. 1110–1125.

Bychkov D.A., Koptev-Dvornikov E.V., Romanova E.S. Verification of the system of thermobarometers-compositometers on experimental and natural material. UDC 552.111: 550.41

M.V. Lomonosov Moscow State University, Faculty of Geology, Moscow (dmibychkov@gmail.com)

Abstract. The development of a system of thermobarometers - compositometers has been completed, which describes the equilibrium minerals - melt in

anhydrous silicate systems in a wide range of temperatures, pressures and compositions of the melt from komatiites to dacites. Thermobarometers-compositometers have been developed both for silicate phases (olivine, plagioclase, clinopyroxene, orthopyroxene, pigeonite), and for ore minerals (magnetite, chrome spinel, ilmenite). In addition, an equation is derived that describes sulfide-silicate liquation.

A joint verification of the algorithm of the CryMinal program and the obtained system of thermobarometers-compositometers based on the material of several experimental series with different order of phase appearance on the liquidus was performed. Verification results demonstrate good agreement between experimental and calculated data.

Keywords: thermobarometer, verification, silicate melt, equilibrium

The main goal of our study is the reconstruction of the processes of formation of large stratified basic-hyperbasitic intrusions. In addition, the study of the processes of formation of layered intrusions can shed light on the problem of magmatic evolution.

In recent decades, a significant part of the efforts of our scientific group has been directed to the derivation of thermobarometers-compositometers to describe the equilibrium between minerals and melt in dry basic-hyperbasite systems in a wide range of melt compositions, temperature, pressure and oxygen fugacity. To date, this work can be considered, to a first approximation, completed, since we have developed thermobarometers-compositometers for silicate minerals: olivine, plagioclase, orthopyroxene, clinopyroxene, pigeonite (Koptev-Dvornikov E.V., Bychkov D.A., 2019; Koptev-Dvornikov E.V., Bychkov D.A., 2018; Koptev-Dvornikov, Bychkov, 2007), as well as ore minerals: magnetite, ilmenite and chrome spinel (Aryaeva et al., 2018; Aryaeva et al., 2016; Chernykh, 2017). In addition, a thermobarometer has been developed that allows one to determine the temperature and content of sulfide sulfur in a melt when sulfide liquid is separated from it (Koptev-Dvornikov et al., 2012).

All developed thermobarometers-compositometers satisfactorily reproduce both the composition of minerals in equilibrium with a silicate melt and the temperature of equilibrium. However, the quality of modeling the equilibrium is determined not so much by the work of each thermobarometer-compositometer individually, but by the general work of the whole complex of thermobarometers-compositometers as a whole.

Verification of the operation of the system of thermobarometers-compositometers was carried out on the basis of a series of quenching experiments with a single starting composition of the system, performed at various temperatures and oxygen fugacity. As an integral characteristic characterizing the deviation of the calculated results from the experimental ones, we chose the sum of the squared deviations of the concentrations of the melt components between the calculation and the experiment.

The results of the first calculations were not entirely satisfactory. Moreover, from the experience of previous calculations, we knew that relatively small deviations in the oxygen fugacity (within the same logarithmic unit) can lead to a noticeable change in the phase composition. Based on this, we decided in the calculations to fix the bulk composition of the system and the temperature of the experiment in accordance with published by authors, and use oxygen fugacity as a fitting parameter.

To demonstrate the results obtained, two series of quenching experiments were selected from the INFOREX database (Ariskin et al., 1992; Ariskin et al., 1997) (all experiment numbers, names of starting compositions and publication numbers are given with the corresponding numbers from the INFOREX database) 236 publication (Tuff, 2005), with experiment numbers 1 to 6 and BAS-1 starting composition, 67 publication (Grove, 1989) , with experiment numbers 26 to 32 and the starting composition of AND-2.

Based on the results of calculations in the CryMinal program, for each starting composition and a certain temperature, a graph was constructed of the dependence of the sum of squares of deviations of the calculated melt composition from the experimental depending on the oxygen fugacity. Optimum oxygen fugacity was considered at which the deviation of the melt composition was minimal.

As a result of applying this approach for work 236, we see (Fig. 1) that the temperatures of the appearance of phases on the liquidus and the proportions of their crystallization are reproduced satisfactorily.

It should be noted that deviations of the composition of the melt were minimized, and the proportions of crystallization of the phases were reproduced without additional efforts of the authors.

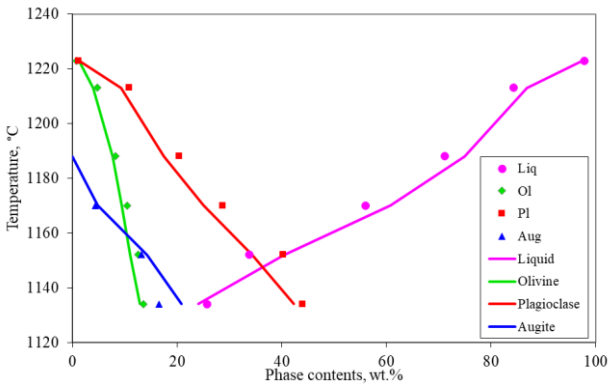

Fig. 1. Experimental (markers) and calculated (lines) phase contents in the experimental series with a starting composition of 236 BAS-1.

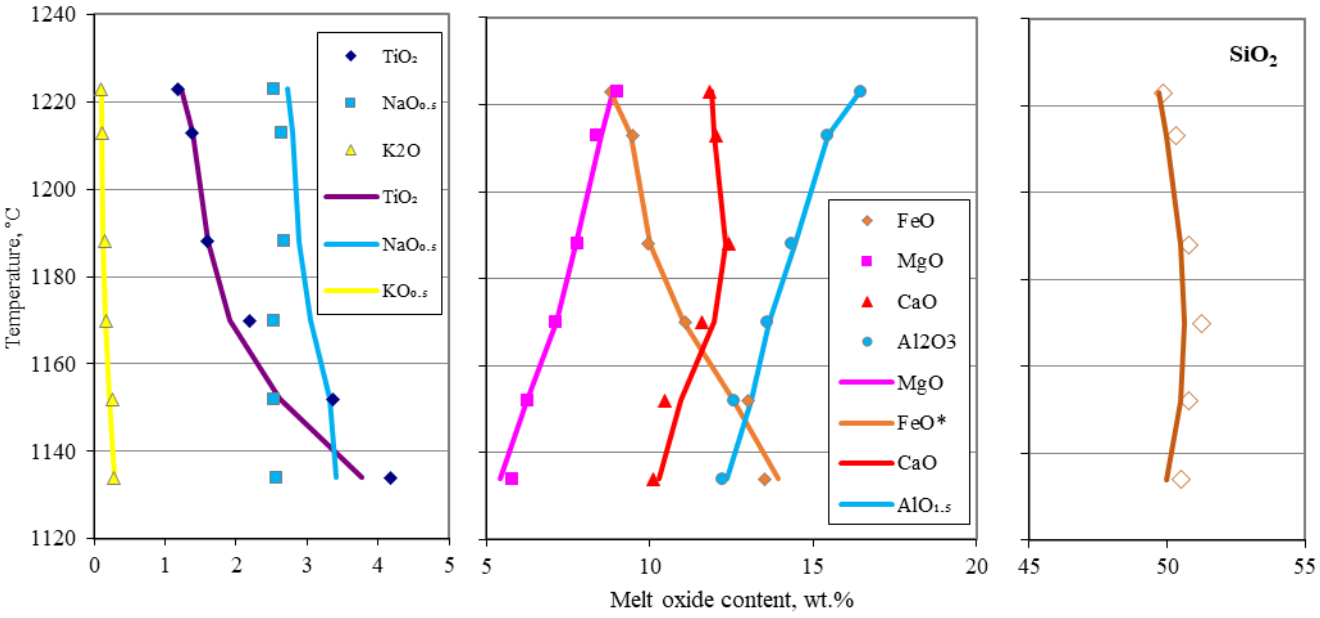

Fig. 2. Experimental (markers) and calculated (lines) oxide contents in melts of the experimental series with a starting composition of 236 BAS-1.

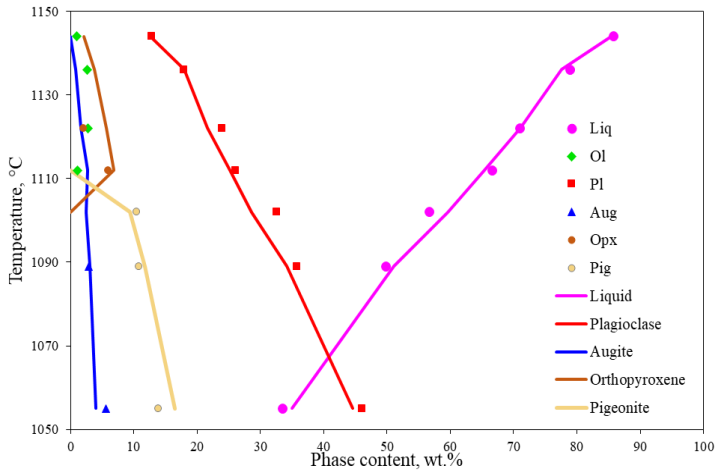

Fig. 3. Experimental (markers) and calculated (lines) phase contents in the experimental series with starting composition 67 ANB-2.

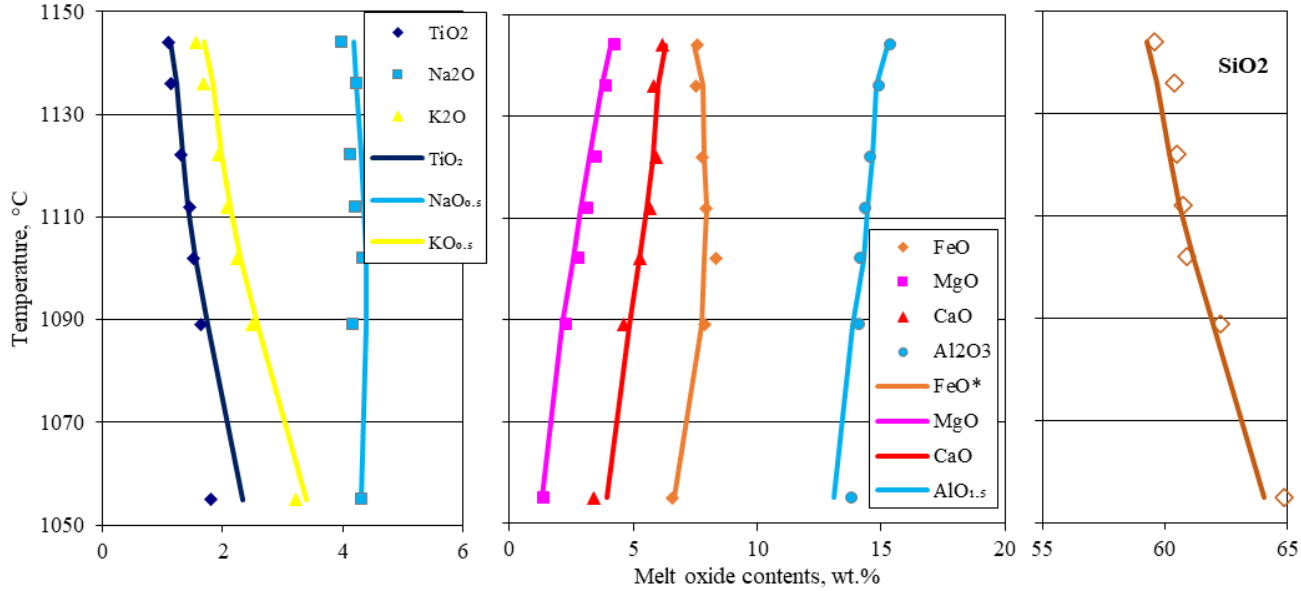

Fig. 4. Experimental (markers) and calculated (lines) oxide contents in melts of the experimental series with starting composition 67 ANB-2.

The calculated melt composition is also well reproduced (Fig. 2). The difference in oxide contents did not exceed 0.6 wt.% for SiO_2, 0.7 wt.% for TiO_2, 0.5 wt.% for Al_2O_3, 0.4 wt.% for FeO, 0.16 wt.% for MnO, 0.39 wt.% for MgO, 0.48 wt.% for CaO, 0.82 wt.% for Na_2O, 0.04 wt.% for K_2O. Moreover, the deviations of the selected oxygen fugacity from the experimental lie in the range from 0.1 to 1.35 logarithmic units.

When verifying calculations on a series of experiments from 67 work with the starting composition of AND-2, it turned out that the contents of plagioclase, augite, and pigeonite are reproduced satisfactorily, however, instead of olivine, orthopyroxene appears from the highest experimental temperatures (Fig. 3). This is the result of the fact that the calculated liquidus of orthopyroxene is several degrees higher in temperature than the liquidus of olivine. At temperatures of 1112°C and below, the phase composition of the system is reproduced very well. Especially noteworthy is the correspondence of the position of the peritectic reaction between orthopyroxene and pigeonite to the experimental one.

The calculated melt composition is also well reproduced (Fig. 4). The deviation of oxide concentrations did not exceed 0.7 wt.% for SiO_2, 0.1 wt.% for TiO_2, 0.3 wt.% for Al_2O_3, 0.45 wt.% for FeO, 0.07 wt.% for MnO, 0.25 wt.% for MgO, 0.34 wt.% for CaO, 0.20 wt.% for Na_2O, 0.15 wt.% For K_2O. Deviations of the selected oxygen fugacity from the experimental lie in the range from 0.07 to 2.99 logarithmic units. Moreover, the largest deviations in the oxygen fugacity are observed for the most high-temperature experiments. A similar pattern manifested itself in other series of calculations.

In general, the complex of thermobarometers-compositometers for silicate minerals has shown its satisfactory performance. The calculated crystallization sequence coincides with that stated in the experiments.

In the series of experiments considered, in some temperature cross sections, instead of olivine, orthopyroxene is present in the calculations. This means that the correct modeling of olivine-orthopyroxene peritectic needs to be tested in more experiments.

The authors are sincerely grateful to the team that created and continuously replenishes the INFEX system for their dedicated work.

References

Ariskin A.A., Bouadze K.V., Meshalkin S.S., Tsekhonya T.I. INFOREX: A database on experimental studies of phase relations in silicate systems // Amer. Mineral. 1992. Vol.77. p.668-669

Ariskin A.A., Meshalkin S.S., Almeev R.R., Barmina G.S., Nikolaev G.S. INFOREX information retrieval system: analysis and processing of experimental data on phase equilibria of igneous rocks. Petrology. - 1997 T. 5. No. 1. S. 32-41.

Aryaeva N. S., Koptev-Dvornikov E. V., Bychkov D. A. Liquid thermobarometer for modeling equilibrium of chrome spinel melt: method of inference and verification // Moscow University Physics Bulletin. Series 4: Geology. - 2016. - No. 4. - S. 30–39.

Aryaeva N.S., Koptev-Dvornikov E.V., Bychkov D.A. Liquid thermobarometer for modeling magnetite – melt equilibrium // Moscow University Physics Bulletin. Series 4: Geology. - 2018. - No. 1. - S. 70–79.

Chernykh N.S. The influence of physico-chemical parameters on the separation of ore phases from basic magmas (according to the results of mathematical modeling): dis. Cand. min-min sciences.- M., 2017.- Access mode: https://istina.msu.ru/download/31973484/1gt8NA:AAlr7ogU29Rp0d-8y3Jqv9TrURs/

Grove T.L., Juster T.C. Experimental investigations of low-Ca pyroxene stability and olivine-pyroxene-liquid equilibria at 1-atm in natural basaltic and andesitic liquids // Contribs Mineral. and Petrol.,1989, V. 103, N3, P. 287-305.

Koptev-Dvornikov E.V., Aryaeva N.S., Bychkov D.A. The thermobarometer equation for the description of sulfide-silicate segregation in basic systems // Petrology. - 2012. - T. 20, No. 5. - S. 1–18.

Koptev-Dvornikov E.V., Bychkov D.A. Geothermometers for a wide range of mafic compositions // Materials of the international conference “Ultrabasite-mafic complexes of folded areas”. Irkutsk: Publishing House of the SB RAS, 2007. P. 178–181.

Koptev-Dvornikov EV, Bychkov D.A. Development of a liquidus thermobarometer for modeling olivine – melt equilibrium // Moscow University Physics Bulletin. Series 4: Geology. - 2019. - No. 5. - S. 62–74.

Koptev-Dvornikov EV, Bychkov D.A. Equations for calculating the content of small components (Fe, Mg, K) in plagioclases, equilibrium with the melt // Transactions of the All-Russian annual seminar on experimental mineralogy, petrology and geochemistry. Moscow, April 18-19, 2018. - GEOCHI RAS, Moscow, 2018. - P. 114–116.

Sano T., Fujii T., Deshmukh S.S., Fukuoka T., Aramaki S. Differen- tiation processes of Deccan Trap Basalts: Contribution from geochemistry and experimental petrology // J. Petrol., 2001, V. 42, N 12, P. 2175-2195.

Tuff J., Takahashi E., Gibson S.A. Experimental constraints on the role of garnet pyroxenite in the genesis of high-Fe mantle plume derived melts // J. Petrol., 2005, V. 46, N 10, P. 2023-2058.

Chevychelov V.Yu. On the solubility of ferrotapiolite and nb/ta ratios in model high-aluminous, subaluminous and alkaline granitoid melts UDC 550.42

D.S. Korzhinskii Institute of Experimental Mineralogy of Russian Academy of Sciences (IEM RAS) Russia, Chernogolovka, Moscow district (chev@iem.ac.ru)

Abstract. The experiments were conducted in internally heated pressure vessels (IHPV) at T = 650, 750 and 850°C, P = 100 MPa and run duration from 5 to 10 days. The alkalinity-aluminous content of granitoid melts has a noticeably less influence on the solubility of ferrotapiolite compared with the solubility of other Ta-Nb minerals studied by us. Although the general form of the dependence on the graph remains the same: for example, the maximum contents of Ta and Nb (up to 2.5 and 0.27 wt.%, respectively) were obtained in alkaline melt with A/CNK =0.7, the contents of these metals decrease (to 0.6 and 0.08 wt.%, respectively) in subaluminous melt (A/CNK =1.1 -1.3) and then slightly change in high-aluminous melt (A/CNK =1.6 -1.9), increasing to 0.76% for Ta and decreasing to 0.04% for Nb. At 850°C, the positive effect of temperature on the solubility of ferrotapiolite is markedly expressed in alkaline melts. When replacing the contents of Ta and Nb in the melt with their partition coefficients between the melt and ferrotapiolite ($^{melt/mineral}D$), we neutralize the differences in the contents of Ta and Nb in the mineral. In this case, the behavior of these two elements practically coincides within the limits of the given errors. The Nb/Ta ratios in the melt at dissolution of ferrotapiolite is significantly lower than at dissolution of tantalite and columbite and is quite close to the magnitude of these ratios at dissolution of microlite. In a first approximation, this correlates with the Nb/Ta ratios in the concerned minerals. It should be noted that in high-aluminous melts (at A/CNK =1.6-1.7), the Nb/Ta ratios in the melt at the dissolution of ferrotapiolite, microlite, and tantalite converge.

Keywords: solubility; ferrotapiolite; experiment; aluminosilicate melts; granitoids; niobium; tantalum

Initial water-saturated model glasses of the SiO_2-Al_2O_3-Na_2O-K_2O composition with additions of 0.5 wt.% CaO and 1 wt.% LiF were prepared by melting from gel mixes. Glasses of three compositions were used in the experiments, differed in aluminium saturation index (mol.Al_2O_3/(CaO+Na_2O+K_2O) = (A/CNK)), respectively about 0.64 (alkaline melt), 1.10 (subaluminous melt) and 1.70 (high-aluminous melt). We also used the natural mineral ferrotapiolite (Sapucaia do Norte, Galileia, Minas Gerais, Brazil, kindly provided by I.V. Pekov) of the following composition (in wt.%): 13.5±0.5 FeO, 6.7±0.6 Nb_2O_5, 77.3±2.3 Ta_2O_5, 1.3±0.5 SnO_2, 0.5±0.3 TiO_2, and 0.7±0.2 MnO. At the preparation of experiments, the powder of model aluminosilicate glass was loaded in Pt capsule, small pieces of crystalline mineral (from one to four) were placed in the center, an excess of 0.1N HF solution (from 16 to 21 wt.%) was added, and then the capsule was welded shut. The experiments were carried out in internally heated pressure vessels (IHPV) at T =650, 750 and 850°C, P =100 MPa and run durations from 5 to 10 days depending on temperature. The experimental conditions and the conditions of the analysis of the obtained products are described in detail in the paper (Chevychelov et al., 2019).

As a result of the experiments, the stability of ferrotapiolite was established when it dissolves in high-aluminous granitoid melts in the entire investigated temperature range. At the same time in alkaline and subaluminous melts at all temperatures, a thin layer is formed on the surface of the mineral, not more than 5-10 mkm thick (Fig. 1). The layer has a composition close to microlite (in wt.%): 3.3 F, 4.9 Na_2O, 11.1 CaO, 6.1 Nb_2O_5, and 72.1 Ta_2O_5; in addition it can contain up to 2.6 FeO, and at 650°C also has up to 5.4 SiO_2 and 0.8 SnO_2. At T = 750 and 850°C granitoid glasses after experiments are amorphous and homogeneous. The high-aluminous glass contains individual acicular crystals of sillimanite-mullite approximately 1×20 mkm in size. At 650°C after experiments, significant crystallization of the glasses was observed with the formation of albite, potassium feldspar, quartz and mica. The maximum degree of crystallization was observed in the subaluminous melt (in some places up to 60-90 wt.% of crystals), the minimum was in the alkaline melt (up to 20-35 wt.%) and intermediate degree was in the high-aluminous melt (up to 60-65 wt.%). To analyze the chemical composition, we chose, whenever possible, the areas of pure non-crystallized glass.

The alkalinity-aluminous content of the granitoid melt has a noticeably less effect on the solubility of ferrotapiolite compared to the solubility of other tantalum-niobates studied by us (Fig. 2). Although the general form of the dependence remains the same: thus, the maximum contents of Ta and Nb, up to 2.5 and 0.27 wt% respectively, were obtained in alkaline melt with A/CNK of about 0.7, the contents of these metals decrease to 0.6 and 0.08 wt% respectively, in subaluminous melt (A/CNK =1.1 -1.3) and then slightly change in high-aluminous melts (A/CNK =1.6 -1.9), increasing to 0.76% for Ta and decreasing to 0.04% for Nb. At 850°C the positive effect of temperature on the solubility of ferrotapiolite is noticeably expressed in alkaline melts. With an increase in the alumina content in the melt, the temperature effect decreases. There are no differences in ferrotapiolite solubility between 750 and 650°C within the margin of error. At a similar form of dependences on the graph, the Ta content (2.5 -0.24 wt.%) in melts is noticeably higher than the Nb content (0.27 -0.01%), which is explained by the difference in the content of these metals in the mineral. By replacing the Ta and Nb contents in the melt with their partition coefficients between the melt and ferrotapiolite ($^{melt/mineral}D$), we level the differences in the Ta and Nb contents in the mineral. In this case (Fig. 3), the behavior of these two elements coefficients on the graph practically coincides within the limits of the given errors.

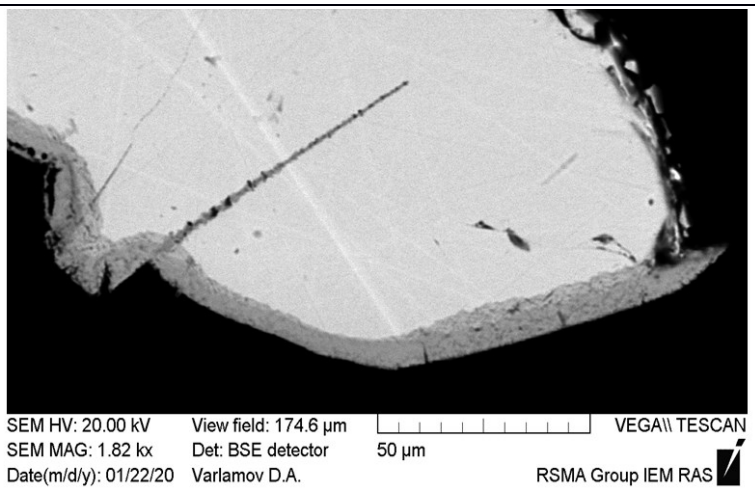

Fig. 1. The layer formed on the surface of ferrotapiolite grain at its dissolution in the alkaline granitoid melt (mol. A/CNK =0.67) at T = 750°C and P =100 MPa.

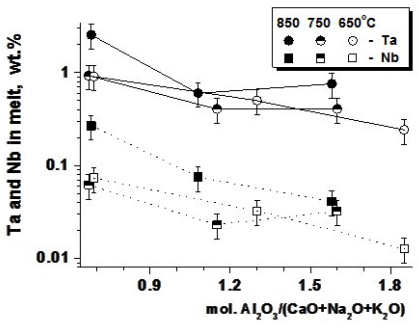

Fig.2.

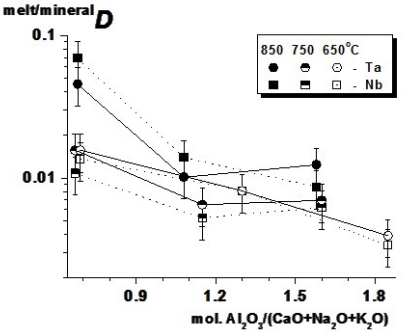

Fig.3.

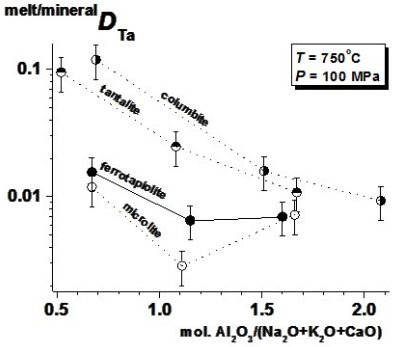

Fig.4.

Fig. 2. Dependences of Ta and Nb contents at dissolution of ferrotapiolite in granitoid melts with various alkalinity-aluminous content at T =650-750-850°C and P =100 MPa.

Fig. 3. Dependences of the partition coefficients of Ta and Nb between granitoid melt and ferrotapiolite ($^{melt/mineral}D$) at mineral dissolution in melts with various alkalinity-aluminous content at T =650-750-850°C and P =100 MPa.

Fig. 4. Dependences of the Ta partition coefficients ($^{melt/mineral}D$) at dissolution of ferrotapiolite in melts with various alkalinity-aluminous content. For comparison our earlier obtained data about the dissolutions of columbite, tantalite and microlite are presented.

Comparison of the obtained data on the solubility of ferrotapiolite in granitoid melts with our earlier results on the dissolution of columbite (Chevychelov et al., 2010; Chevychelov, 2013), tantalite (Chevychelov, 2016), and microlite (Chevychelov et al., 2019) at similar conditions shows (Fig. 4) that for ferrotapiolite the dependence of the Ta partition coefficients is close to the dependence shown on the graph for microlite in the field of alkaline and subaluminous melts and is located noticeably below the dependence lines for columbite and tantalite. It can be assumed that the closeness of these dependences for ferrotapiolite (tetragonal crystal system) and microlite (cubic crystal system) is associated with the similarity of bonds and the arrangement of Ta in their crystal structures and their difference from the position of Ta in the crystal structure of columbite-tantalite (rhombic crystal system). In high-aluminous melt (A/CNK ≥1.6 -1.7), the Ta partition coefficients for all four minerals on the graph converge.

Nb/Ta ratios in the melt at dissolution of ferrotapiolite are significantly lower than at dissolution of tantalite and columbite and are quite close to the values of these ratios at dissolution of microlite (Fig. 5). To a first approximation, this regularity correlates with the Nb/Ta ratios in the minerals under consideration. It should be noted that in high-aluminous melts (A/CNK =1.6-1.7) Nb/Ta ratios in the melt approach each other at dissolution of ferrotapiolite, microlite, and tantalite.

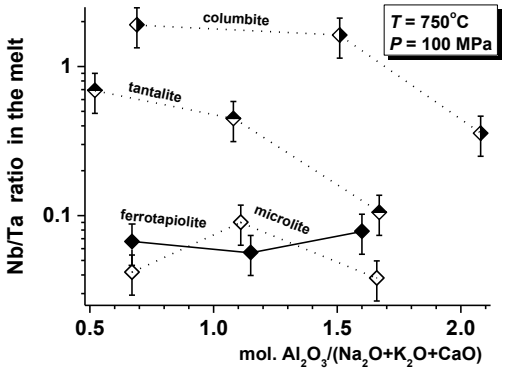

Fig. 5. Nb/Ta ratios in aluminosilicate melts with various alkalinity-aluminous content at dissolution of

ferrotapiolite. For comparison our earlier data about the dissolutions of columbite, tantalite and microlite are presented.

Acknowledgments. *The author is grateful to I.V. Pekov for the kindly provided samples of ferrotapiolite. This* study *was* financially *supported by the Russian Foundation for Basic Research,* project No *18-05-01001A.*

References

Chevychelov V.Yu. Partitioning of volatile, rock-forming and ore components in magmatic systems: experimental studies: Author's abstract dis. doctor geol.-min. sciences. – Moscow, 2013. - 62 p. (in Russian)

Chevychelov V.Yu. Experimental study of the dissolution of columbite and tantalite-columbite in water-saturated granitoid melts // Sofia Initiative Preservation of Mineral Diversity. VIII International Symposium Mineral diversity research and preservation. Earth and Man National Museum, - Sofia, Bulgaria, 2016. - P. 22-34. (in Russian)

Chevychelov V.Yu., Borodulin G.P., Zaraisky G.P. Solubility of columbite, $(Mn,Fe)(Nb,Ta)_2O_6$, in granitoid and alkaline melts at 650-850°C and 30-400 MPa: an experimental investigation // Geochemistry International. - 2010. – Vol. 48, № 5. - P. 456-464. (in English)

Chevychelov V.Yu., Viryus A.A., Shapovalov Yu.B. Dissolution of pyrochlore and microlite in alkaline, sub-aluminous and high-aluminous granitoid melts // Doklady Earth Sciences. - 2019. - Vol. 489, Part 2. - P. 1465-1468. (in English)

Chevychelov V.Yu., Viryus A.A. Solubility of ilmenorutile in model granitoid melts at various alkalinity–alumina. UDC 550.42

D.S. Korzhinskii Institute of Experimental Mineralogy of Russian Academy of Sciences (IEM RAS) Russia, Chernogolovka, Moscow district (chev@iem.ac.ru)*, (mukhanova@iem.ac.ru), +7(962)971-25-14*

Keywords solubility; ilmenorutile; experiment; aluminosilicate melts; granitoids; niobium; titanium

Abstract. The experiments were conducted in internally heated pressure vessels (IHPV) at T = 650, 750 and 850°C, P = 100 MPa and run duration from 5 to 10 days. The maximal influence on ilmenorutile dissolution in granitoid melts is exerted by the alkalinity-aluminous content of the melt. Thus, the highest Nb contents (up to 1.2 wt.%) were obtained in alkaline melts (aluminium saturation index, mol. $Al_2O_3/(CaO+Na_2O+K_2O)$ =A/CNK =0.7-0.6), the Nb contents were decreased to ≈0.2 -0.1 wt.% in subaluminous melts (A/CNK =1.1) and then still decrease to ≈0.1 -0.02 wt.% in high-aluminous melts (A/CNK =1.6 -1.9). An increase in temperature has a noticeable positive effect on the Nb content in alkaline melts, but in subaluminous and high-aluminous melts, the highest Nb contents were obtained at T =750°C, and they decrease both at 850 and 650°C. The Ti contents at dissolution of ilmenorutile in the same melts change like Nb. When replacing the contents of Nb and Ti in the melt with their partition coefficients between the melt and ilmenorutile ($^{melt/mineral}D$), we neutralize the differences in the contents of Nb and Ti in the mineral. In this case, the behavior of these two elements practically coincides within the limits of the given errors. A comparison of the data on the solubility of ilmenorutile in granitoid melts with our earlier results on the dissolution of columbite, tantalite and pyrochlore at similar conditions shows that the dependence of the Nb partition coefficients of ilmenorutile falls into the field on the graph formed by such dependences for columbite and tantalite. Only in the high-aluminous melt the slightly higher $^{melt/mineral}D_{Nb}$ coefficient of ilmenorutile was obtained.

Initial water-saturated model glasses of the SiO_2-Al_2O_3-Na_2O-K_2O composition with additions of 0.5 wt.% CaO and 1 wt.% LiF were prepared by melting from gel mixes. Glasses of three compositions were used in the experiments, differed in aluminium saturation index (mol.$Al_2O_3/(CaO+Na_2O+K_2O)$ = (A/CNK)), respectively about 0.64 (alkaline melt), 1.10 (subaluminous melt) and 1.70 (high-aluminous melt). We also used the natural mineral ilmenorutile (Selyankina village, Ilmenskie mountains, South Ural, kindly provided by I.V. Pekov) of the following composition (in wt.%): 77.6±1.8 TiO_2, 7.6±0.7 Fe_2O_3, and 14.8±0.9 Nb_2O_5. At the preparation of experiments, the powder of model aluminosilicate glass was loaded in Pt capsule, one rather large fragment of the crystalline mineral was placed in the center, an excess of 0.1N HF solution (from 16 to 22 wt.%) was added, and then the capsule was welded shut. The experiments were carried out in internally heated pressure vessels (IHPV) at T =650, 750 and 850°C, P =100 MPa and run durations from 5 to 10 days depending on temperature. The experimental conditions and the conditions of the analysis of the obtained products are described in detail in the paper (Chevychelov et al., 2019).

As a result of the experiments, the stability of ilmenorutile was established when it dissolves in subaluminous and high-aluminous granitoid melts in the entire investigated temperature range. At the same time in alkaline melt at 850°C, a layer, about 20 mkm thick, is formed on the surface of the mineral (Fig. 1), which additionally includes 3.4 wt.% SiO_2, 0.8% Al_2O_3, 0.3% K_2O and in which the Nb_2O_5 and Fe_2O_3 contents decrease to 9.7% and 5.1%, respectively. At 750°C in alkaline melt, the surface of ilmenorutile was covered with a thin 10–20 mkm layer consisting of titanite (in wt.%): 2.4 Na_2O, 23.4 CaO, 38.1 TiO_2, 6.8 Nb_2O_5, and 29.3 SiO_2. At T =750 and 850°C granitoid glasses after experiments

are amorphous and homogeneous. The high-aluminous glass contains individual acicular crystals of sillimanite-mullite approximately 1×20 mkm in size. At 650°C after experiments, significant crystallization of the glasses was observed with the formation of albite, potassium feldspar, quartz and mica. The maximum degree of crystallization was observed in the subaluminous melt (in some places up to 90-95 wt.% of crystals), the minimum was in the high-aluminous melt (up to 35-40 wt.%) and intermediate degree was in the alkaline melt (up to 40-65 wt.%). To analyze the chemical composition, we chose, whenever possible, the areas of pure non-crystallized glass.

The alkalinity-aluminous content of the melt has the greatest effect on the solubility of ilmenorutile in granitoid melts (Fig. 2). Thus, the maximum Nb contents (up to 1.2 wt.%) were obtained in alkaline melt with aluminum saturation index A/CNK of about 0.7 -0.6, the Nb contents decrease to 0.2 -0.1 wt.% in subaluminous melts (A/CNK =1.1) and then decrease even further to 0.1-0.02 wt.% in high-aluminous melt (A/CNK is about 1.6-1.9). An increase in temperature has a noticeable positive effect on the Nb content in alkaline melts, but in subaluminous and high-aluminous melts, the highest Nb contents are obtained at T =750°C, and they decrease at both 850 and 650°C. The Ti content at ilmenorutile dissolution in the same melts changes like Nb. Due to the higher Ti content in ilmenorutile, the absolute values of Ti content in the melt are significantly higher than Nb (2.7–1.6 wt.% in alkaline melt, 0.6–0.5% in subaluminous melt, and 0.8–0.2% in high-aluminous melt). By replacing the Nb and Ti contents in the melt with their partition coefficients between the melt and ilmenorutile ($^{melt/mineral}D$), we level the differences in the Nb and Ti contents in the mineral. In this case (Fig. 3) the behavior of these two elements coefficients on the graph practically coincides within the limits of the given errors.

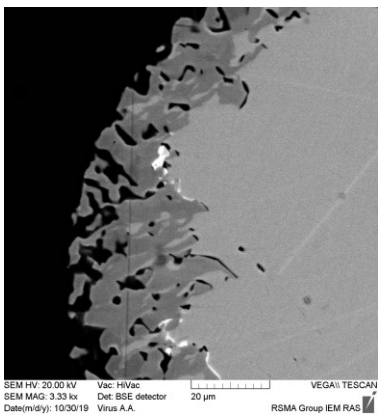

Fig. 1. The layer formed on the surface of ilmenorutile grain at its dissolution in alkaline granitoid melt (molar A/CNK =0.72) at T = 850°C and P =100 MPa.

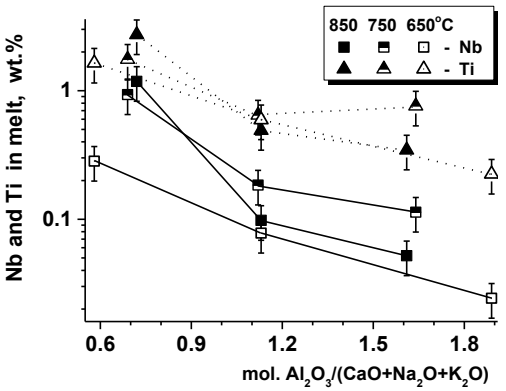

Fig.2. Dependences of Nb and Ti contents at ilmenorutile dissolution in granitoid melts with various alkalinity-aluminous content at T =650-750-850°C and P =100 MPa.

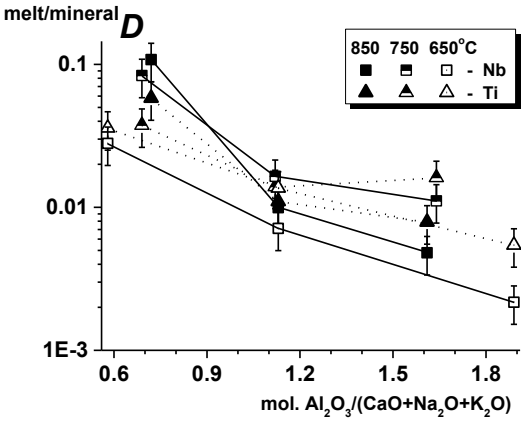

Fig. 3. Dependences of the partition coefficients of Nb and Ti between granitoid melt and ilmenorutile (melt/mineralD) at mineral dissolution in melts with various alkalinity-aluminous content at T =650-750-850°C and P =100 MPa.

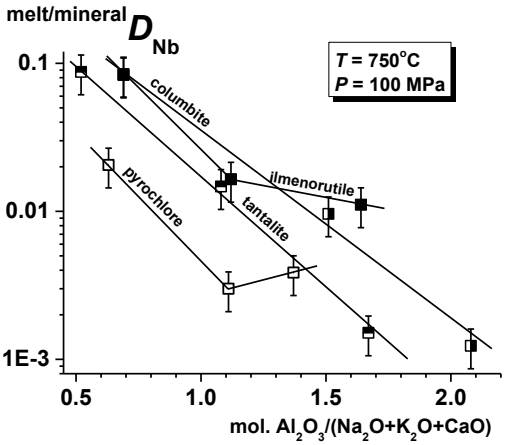

Fig. 4. Dependences of the partition coefficients of Nb ($^{melt/mineral}D$) at ilmenorutile dissolution in melts with various alkalinity-aluminous content. For comparison our earlier data about the dissolutions of columbite, tantalite, and pyrochlore are presented.

Comparison of the obtained data on the solubility of ilmenorutile in granitoid melts with our earlier results on the dissolution of columbite (Chevychelov et al., 2010; Chevychelov, 2013), tantalite (Chevychelov, 2016), and pyrochlore (Chevychelov et al., 2019) at similar conditions shows (Fig. 4) that for ilmenorutile the dependence of the Nb partition coefficients falls on the given graph in the field formed by such dependences for columbite and tantalite. The slightly higher $^{melt/mineral}D_{Nb}$ coefficient was obtained for ilmenorutile only in the high-aluminous melt. At the same time, the type and position on the graph of such dependence of pyrochlore is noticeably different from the others. The values of the $^{melt/mineral}D_{Nb}$ coefficients for pyrochlore with similar alkalinity-aluminous content of the melt are noticeably lower than for other considered minerals. High-aluminous melt is exception, in which the Nb partition coefficient at pyrochlore dissolution increases relative to subaluminous melt, though at other minerals dissolution the Nb coefficient decreases from subaluminous to high-aluminous melt. Probably, these regularities can be associated with the similarity of bonds and the arrangement of Nb in the crystal structures of ilmenorutile (tetragonal crystal system) and columbite-tantalite (rhombic crystal system) and their difference from the position of Nb in the crystal structure of pyrochlore (cubic crystal system).

Acknowledgments. *The authors are grateful to I.V. Pekov for the kindly provided samples of ilmenorutile. This* study *was* financially *supported by the Russian Foundation for Basic Research,* project No *18-05-01001A.*

References

Chevychelov V.Yu. Partitioning of volatile, rock-forming and ore components in magmatic systems: experimental studies: Author's abstract dis. doctor geol.-min. sciences. – Moscow, 2013. - 62 p. (in Russian)

Chevychelov V.Yu. Experimental study of the dissolution of columbite and tantalite-columbite in water-saturated granitoid melts // Sofia Initiative Preservation of Mineral Diversity. VIII International Symposium Mineral diversity research and preservation. Earth and Man National Museum, - Sofia, Bulgaria, 2016. - P. 22-34. (in Russian)

Chevychelov V.Yu., Borodulin G.P., Zaraisky G.P. Solubility of columbite, $(Mn,Fe)(Nb,Ta)_2O_6$, in granitoid and alkaline melts at 650-850°C and 30-400 MPa: an experimental investigation // Geochemistry International. - 2010. – Vol. 48, № 5. - P. 456-464. (in English)

Chevychelov V.Yu., Viryus A.A., Shapovalov Yu.B. Dissolution of pyrochlore and microlite in alkaline, sub-aluminous and high-aluminous granitoid melts // Doklady Earth Sciences. - 2019. - Vol. 489, Part 2. - P. 1465-1468. (in English)

Khodorevskaya L.I. Experimental modelling of alkaline metasomatism under pressure gradient conditions at 750°C. UDC 553.065.1

D.S. Korzhinskii Institute of Experimental Mineralogy RAS, Chernogolovka Moscow district. (khodorevskaya@mail.ru).

Abstract. Compositions and specificity of formation of metasomatic minerals at conditions of Si, Ca and Mg transportation by alkaline solutions were studied. Gradients of temperature and pressure were created in an ampulla at external T=750 °C and P=500 MPa. At these conditions and presence of fluid H_2O-Na_2CO_3 (X_{Na2CO3} = 0.07), diopside was dissolved, solutes were transtported to and precipitated on amphibolite. This resulted in formation of alkaline asociations of Na-Ca amphibole, similar to cataphorite, aegirine, aegirine-augite, nepheline on the amphibolite surface. It was shown previously that aegirine and nepheline are not formed at less content of the salt in the fluid (X_{Na2CO3} = 0.035). Accordingly, appearance of aegirine and nepheline evidences increasing of fluid alkalinity, in particular, increasing X_{Na2CO3} to values exceeding 0.05.

Keywords*: aegirine; aegirine-augite; amphibole; katophorite; nepheline; alkaline metasomatism; fluid.*

A great variety of alkaline metasomatic rocks from phenites associated with plutonic alkaline complexes and carbonatites to low-temperature alkaline rocks is largely dependent on the presence of fluids filtering along circulation zones. Therefore, fluid phase composition is studied to assess conditions for the fluid mobilization and transport of large-ion lithophile (LILE), high-charge (HFSE) and rare-earth (REE) elements characteristic of alkaline rocks.

The genesis of alkaline metasomatic rocks is largely dependent on Na regime. Na activity in alkaline fluids is essential as it is responsible for the evolution of alkaline metasomatic rocks such as albite, aegirine, as well as Ca-Na and Na-amphiboles. These minerals are important indicators of carbonatites; metasomatic rocks themselves occasionally host rare-metal (Nb, Zr, REE) mineralization (Savelyeva et al. 2017; Korchak, 2008; Melgarejo et al., 2012; Chakhmouradian et al., 2015 et al.).

The experimental study of phase relations indicate the leading role of the ligands F^-, Cl^-, PO_4^{3-} and SO_4^{2-} in fluids upon the transfer of HFSE and REE during contact metasomatism (Arzamastsev et al., 2011;). Furthermore, sodium carbonate fluids play an important role in alkaline metasomatism (Kushev, 1972; Savelyeva et al., 2018; et al.).

The results of the modeling of the transfer of petrogenic components by the fluid Na_2CO_3-H_2O (X_{Na2CO3}=0.035) at preset external parameters (T=750°C, P=500 MPa) under P-T gradient conditions created inside an ampoule were reported in (Khodorevskaya, 2019). Diopside was used as the source of transferred Si, Ca and Mg in the experiments. During the experiments diopside was partly dissolved under gradient conditions. Some of dissolved substances remained in solution, while others precipitated on the substrate as an amphibole

rim. Newly-formed amphibole was Mg-cataphorite (Mg-*Ktp)* with an iron content (*f*) of 0.27-0.05.

However, alkaline pyroxenes, which were not obtained in the experiments, commonly occur together with sodium-calcium and sodium amphiboles in natural alkaline metasomatic rocks. This seems to be due to low salt (Na_2CO_3) concentration in the fluid. Therefore, this project is a continuation of studies conducted under gradient conditions at 750°C and at higher salt concentrations in the fluids (X_{Na2CO3}=0.07).

After the experiments, newly-formed minerals, occurring as a continuous or discontinuous rim, were revealed in some portions of the margin of fluid-facing *Grt*-amphibolite (Fig. 1). The rim varied in thickness from 0 to over 500 μm. The newly-formed minerals in the rim are shown in more detail in Fig. 2.

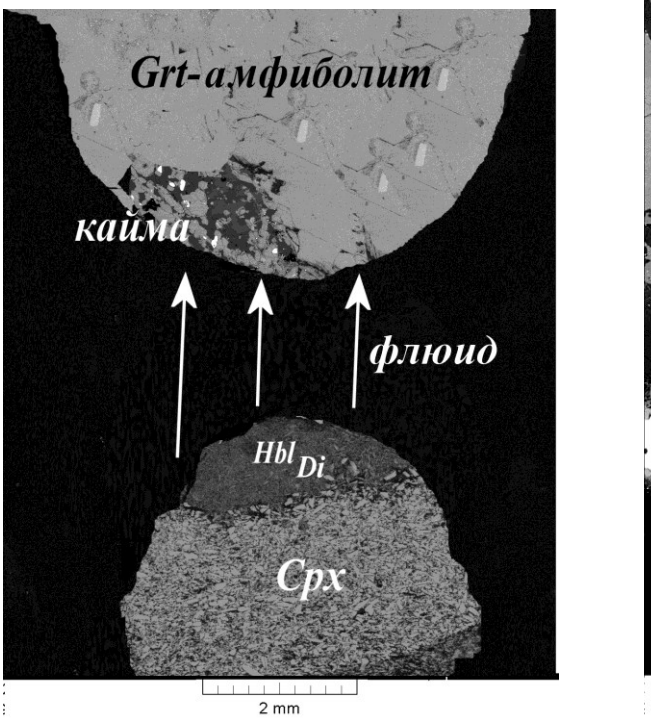

Fig. 1. The scheme of the experiment. The arrows indicate the direction of fluid transfer from diopside to *Grt*-amphibolite.

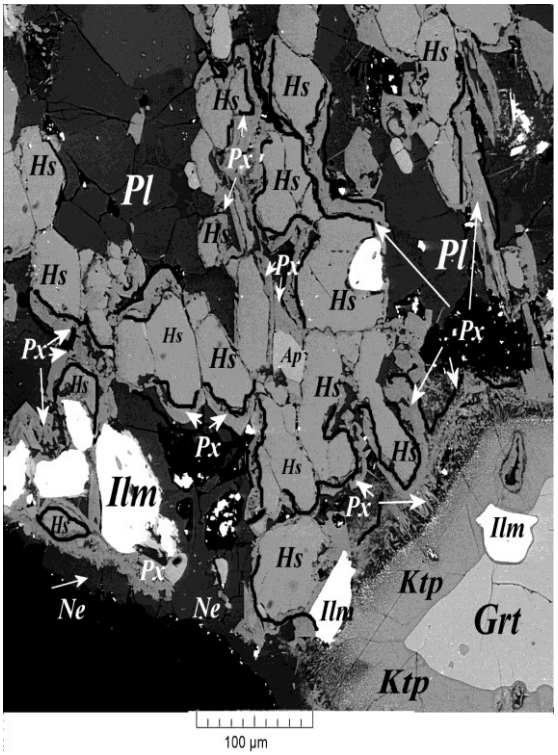

Fig. 2. Newly-formed mineral rim. The black line indicates narrow aegirine-augite rims along amphibole margins.

The fluid-facing margin of amphibolite (Fig. 2) has a discontinuous nepheline rim with an excess of SiO_2 up to 0.22 and FeO impurity up to 0.05. Plagioclase, similar in composition, occurs both in the middle of the sample and at the contact with the fluid (An_{20}). Obviously, felsic plagioclase from amphibolite remains stable in the contact zone.

The amphiboles that make up *Grt* amphibolite occurred as hastingsite (*Hs*) with f = 0.55. *Hs* persisted in the fluid contact zone after the experiments (Fig. 2); iron concentration increased to f = 0.62 from the centre to grain margins.

Narrow, 10 μm thick, well-defined newly-formed pyroxene rims (in Fig. 2, *Px* rims are indicated by a black line) formed along the *Hs* margins. The clinopyroxene is consistent in composition with aegirine and aegirine-augite (Fig. 3). The mineral is rich in FeO (≈ 22-25 mas.%) and TiO_2 (a few per cent). The iron content of the mineral f = 0.70-0.80.

The composition of partly preserved garnet is enriched in almandine from the centre to grain margins, varying from $Grs_{13}Alm_{68}Prp_9Sps_7$ to $Grs_{12}Alm_{75}Prp_8Sps_7$.

A ≈ 50 μm wide rim was formed along the garnet margins. Recalculation of the chemical composition of this mineral for the formula of amphibole is consistent with the values $(_{Na0.6\text{-}0.9}K_{0.1}Ca_{0.05})(Mg_{2.4\text{-}2.6}Fe_{0.2}Ti_{0.1}Al_{0.2})(Si_{2.8}Al_{1.2}O_{10})$ $(OH)_2$. The mineral is the closest in composition and cation ratio to sodium-calcium amphiboles - cataphorites (*Ktp*, Figs. 2 and 4). However, the mineral contains more Na than the cataphorites. Too high Na concentrations in this mineral could be due to the excess of fluid relative to the sample and high Na concentrations in the fluid. Na seems to be adsorbed as part of film solutions on the mineral surface.

$(Al^{VI}+Ca) – (Si+Na+K)$ ratios in the amphiboles, obtained at both X_{Na2CO3}=0.035 and X_{Na2CO3}=0.07 in the fluid, are similar (Fig. 4). However, the newly-formed amphiboles, obtained in more salty fluids, are much richer in iron (f = 0.80).

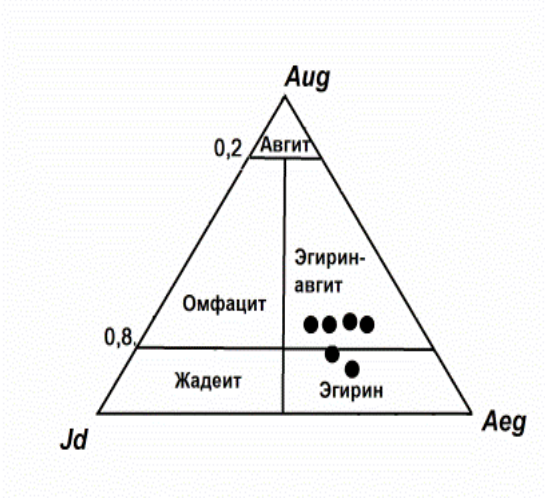

Fig. 3. The compositions of pyroxenes formed in the experiments

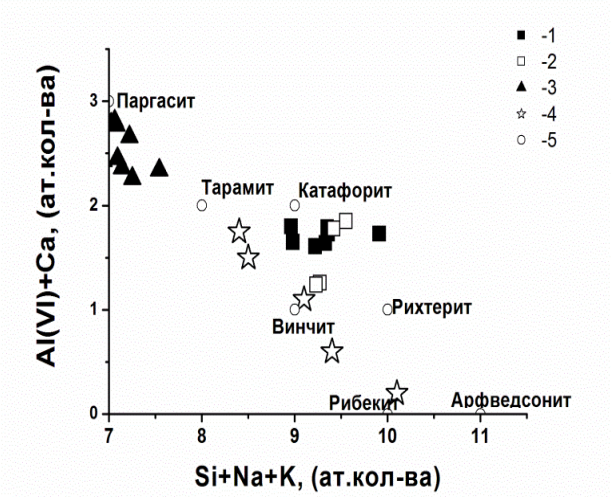

Fig. 4. Compositional characteristics of *Hbl* produced in the experiments: 1-2 – respectively experiments with X_{Na2CO3}=0.035 and X_{Na2CO3}=0.07 in fluid; 3-X_{NaCl}=0-0.45 (Khodorevskaya, Aranovich, 2016; 4 – data (Savelyeva et al., 2017; 5 - end members of *Hbl* according to (Leake et al., 1997).

Triangles in Fig. 4 show amphibole compositions formed at varying NaCl concentrations in the fluid (Khodorevskaya & Aranovich, 2016). One can see that it is the increasing alkalinity of the fluid that is responsible for variations in amphibole composition. Near-neutral solutions are responsible for the presence of edenites and pargasite-hastingsites. As the alkaline content of the solutions increases ($X_{Na2CO3}\approx$ 0.03-0.1), cataphorites are formed. Riebeckites and arfvedsonites seem to form at higher alkalinity.

Thus, the experiments show that minerals, characteristic of alkaline metasomatic rocks, are formed if Na_2CO_3 is present as part of the fluid phase. Na-Ca amphibole – cataphorite with f = 0.05-27 is formed at relatively low salt concentrations (X_{Na2CO3} = 0,035). As fluid salinity increases (X_{Na2CO3} = 0.07), aegirine, aegirine-augite and nepheline are formed together with cataphorite. Newly-formed aegirine and cataphorite contain practically identical high iron concentrations (f = 0.80).

The above experimental studies, as well as the data reported in (Khodorevskaya, 2019), indicate that the removal of elements, dependent on the composition of the fluid phase, including its anion constituent, takes place when T-P parameters display a gradient. The largely aqueous fluid, as well as low chloride (H^+, Na^+, K^+) concentrations contribute to the removal of Ca, Fe and Mg from host rocks. As NaCl concentration in the fluid rises ($X_{NACl}\approx$ 0.1), Fe and Mg are removed from the host rocks, while Ca behaves like an inert constituent. Largely aqueous fluids with small amounts of salt added are responsible for the formation of basificates in granitization processes. High iron concentrations in dark-coloured minerals and the abundance of magnetite and hematite in the basificates are observed, because more iron and less Ca and Mg are removed from host rocks. The presence of carbonate ions in the solutions results in the removal of SiO_2 and CaO (Khodorevskaya, 2019) and lesser Fe from the rocks and inert Mg. Thus, the presence of carbonatites with no visible relation to alkaline-basic magmatite series could be due to the presence of sodium carbonate fluids responsible for the removal of Ca from host rocks and its redeposition into carbonates.

This study was carried out under government-financed project AAAA-A18-118020590148-3 for the Korzhinskii Institute of Experimental Mineralogy, Russian Academy of Sciences, in 2019–2020

References

Arzamastsev A.A., Arzamastseva A.A. Zaraisky G.P. Contact interaction of agpaite magmas with gneisses of the base on the example of Khibinsky and Lovozersky massifs.// Petrologia 2011. № 2. — P. 115–139.

Korchak Yu.A. Mineralogy of rocks of Lovozersky suit and products of their contact-metasomatic transformation in alkaline massifs.: doctor's of sciences theses— Sankt Petersburg, 2008. — 18 p.

Savel'eva V.B., Bazarova E.P., Sharygin V.V., Karmanov N.S. Kanakin S.V. Metasomatites of Ongurensky carbonatite complex (Western Transbaikalia): geochemistry and composition of accessory minerals // Geology of ore deposits. — 2017. № 4. — P. 319–346.

Kushev V.G. Alkaline metasomatites of Pre-Cambrian. — Leningrad, 1972. —190 p

Khodorevskaya L.I. Experimental study of diopside interaction with fluid H_2O-Na_2CO_3 under the conditions of pressure gradient at 750°C //

Proceedings of yearly meeting on experimental mineralogy, petrology and geochemistry— Moscow 2019. — P. 122-125.
Khodorevskaya L.I. Granitization and high temperature metasomatism in rocks of basic composition: comparison of experimental and natural data // Petrology. — 2019б. № 5. — P. 557-576.
Chakhmouradian A.R., Reguir E.P., Kressal R.D. et al. Carbonatite-hosted niobium deposit at Aley, northern British Columbia (Canada): mineralogy, geochemistry and petrogenesis // Ore. Geol. Rev. — 2015. V. 64. — P. 642–666.
Leake B.E., Woolley A.R., Birch W.D. et al. Nomenclature of amphiboles. Report of the Subcommittee on Amphiboles of the International Mineralogical Association Commission on New Minerals and Mineral Names // Eur. J. Mineral. — 1997. V. 9. — P. 623–651.
Melgarejo J.C., Costanzo A., Bambi A.C.J.M. et al. Subsolidus processes as a key factor on the distribution of Nb species in plutonic carbonatites: The Tchivira case, Angola // Lithos. — 2012. V. 152. P. — 187–201.

Koptev-Dvornikov E.V., Romanova E.S., Bychkov D.A. Orthopyroxene liquidus thermobarometer-compositometer for a range of melt compositions from magnesian basites to dacites

M.V. Lomonosov Moscow State University, Department of Geology, Moscow (ekoptev@geol.msu.ru)

Abstract. The results of 354 "dry" quenching experiments (201 of them are high-pressure up to 23 kbar) characterizing the compositions of coexisting orthopyroxenes and melts were extracted from the INFOREX database. The orthopyroxene compositions were recalculated to 9 end-members: $MgSiO_3$ (En – enstatite), $FeSiO_3$ (Fs – ferrosilite), $CaSiO_3$ (Wo – wollastonite), $FeAlO_3$ (FeAl – ferral), $AlAlO_3$ (AlAl – alal), $Na_{0.5}Al_{0.5}SiO_3$ (Jd – jadeite), $MgTiO_3$ (MgTi – magti), $MnSiO_3$ (Rdn – rhodonite), $CrSiO_3$ (CrPx – chrompyroxene).

Thus, orthopyroxene liquidus thermobarometer represents a system of 9 equations, for example, for En:

$$X^{En} = \exp\left(A/T + \beta P/T + B + D\lg f_{O_2} + \sum J_i X_i + \ln a^l_{MgO} + \ln a^l_{SiO_2}\right), \quad (1)$$

where P is the pressure in kbar, T is the absolute temperature, f_{O_2} is the oxygen fugacity, X_i is the molar fraction of the i-th component of the melt, A, β, D, J_i are the coefficients at the corresponding variables, B is the constant, a^l_i is the activity of the components in the melt according to the two-lattice model of silicate liquid of Nielsen with co-authors. In the temperature range from 1050 до 1500ºC, with a 95% probability, the calculated value of the liquidus temperature of orthopyroxene differs from the unknown true temperature by an amount not exceeding ± 5 degrees.

Keywords: orthopyroxene, silicate melt, equilibrium, equation, thermobarometer, modeling.

In order to develop a system of equations intended for modeling the equilibrium of orthopyroxenes with a melt, the results of 354 "dry" quenching experiments (including 201 high-pressure ones) were processed using multidimensional statistics. Each experiment is characterized by temperature, pressure, oxygen fugacity, and phase compositions. The range of melt compositions from magnesian basalts to dacites (Fig. 1). Data extracted from the INFOREX database (Ariskin et al., 1997).

The task was to derive equations that could predict the composition of orthopyroxene, including the contents of small components, in a wide range of compositions of basite systems. After reviewing a number of approaches to accounting for the composition of the system when calculating the equilibrium constant, (E. V. Koptev-Dvornikov and D. A. Bychkov (Koptev-Dvornikov, Bychkov, 2007) settled on the following form of the equation:

$$\ln K = \frac{A + \beta P}{T} + B + D\lg f\mathrm{O}_2 + E\ln\left(\frac{\mathrm{Al}}{\mathrm{Si}}\right) + FW + \sum_{i=1}^{n} J_i X_i \quad (1)$$

where K is the reaction constant for the formation of a minal of any crystalline phase; P is the pressure in kbar; T is the absolute temperature; $f\mathrm{O}_2$ is the oxygen fugacity in bars, $W=\ln((\mathrm{Na+K})\mathrm{Al}/\mathrm{Si}^2)$, X_i is the molar fraction of the i-th component of the melt, and n is the number of components considered.

The parameters Al/Si and W (they are calculated using atomic amounts of elements) are proposed (Ariskin, Barmina, 2000) for the refinement of olivine and plagioclase thermobarometers, respectively. A, β, D, E, F, J_i are coefficients for the corresponding variables, B is a constant. The basis for finding these coefficients is the principle of using methods of multidimensional statistics. The thermodynamic meaning of these constants follows from the form of the known physicochemical equations: $A \sim \Delta H/R$, $\beta \sim -\Delta V/R$, $\{B + D\lg f\mathrm{O}_2 + E\ln\left(\frac{\mathrm{Al}}{\mathrm{Si}}\right) + FW + \sum_{i=1}^{n} J_i X_i\} \sim -\Delta S/R$, где ΔH, ΔV and ΔS are the enthalpy, volume and entropy effects of the phase reaction, R is the universal gas constant.

Traditionally, the composition of orthopyroxene count on three end-member – ferrosillite, enstatite and wollastonite. However, both in natural samples and in experimental orthopyroxenes, microprobe analysis reveals the presence of TiO_2, Al_2O_3, MnO, Na_2O, Cr_2O_3 in amounts reaching the first percent. In this regard, we recalculated the chemical compositions of orthopyroxenes into 9 minals – enstatite $MgSiO_3$ (En), ferrosilite $FeSiO_3$ (Fs), wollastonite $CaSiO_3$ (Wo), feral $FeAlO_3$ (FeAl), alal $AlAlO_3$ (AlAl), jadeite $Na_{0.5}Al_{0.5}SiO_3$ (Jd), Magti $MgTiO_3$ (MgTi), rhodonite $MnSiO_3$ (Rdn), chrompyroxene $CrSiO_3$ (CrPx).

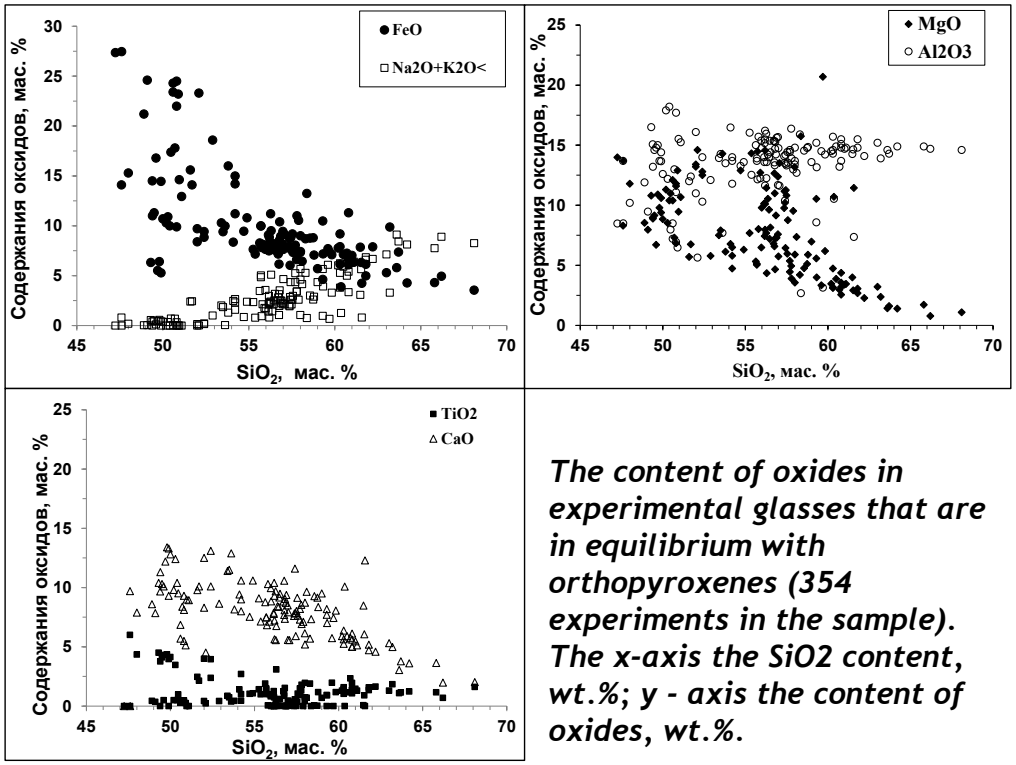

The content of oxides in experimental glasses that are in equilibrium with orthopyroxenes (354 experiments in the sample). The x-axis the SiO2 content, wt.%; y - axis the content of oxides, wt.%.

Fig. 1. Compositions of experimental melts.

The formation of the above mentioned minals from the melt is described by the following heterophase reactions:

$MgO^l + SiO_2{}^l = MgSiO_3$	(En)	
$FeO^l + SiO_2{}^l = FeSiO_3$	(Fs)	
$CaO^l + SiO_2{}^l = CaSiO_3$	(Wo)	
$FeO^l_{1,5} + AlO^l_{1,5} = FeAlO_3$	(FeAl)	(2)
$AlO^l_{1,5} + AlO^l_{1,5} = AlAlO_3$	(AlAl)	
$0{,}5NaO^l_{0,5}+0{,}5AlO^l_{1,5}+SiO^l{}_2=Na_{0,5}Al_{0,5}SiO_3$	(Jd)	
$MgO^l + TiO^l_2 = MgTiO_3$	(MgTi)	
$MnO^l + SiO^l_2 = MnSiO_3$	(Rdn)	
$CrO^l + SiO_2{}^l = CrSiO_3$	(CrPx)	

Expressions for calculating the content of orthopyroxene minals in the mineral follow from the form of equation (1) and reactions (2).

Example for the enstatite end-member:

$$X_{En} = \exp\left[\frac{\left(A_{En}+\beta_{En}P\right)}{T} + B_{En} + D_{En}\lg f_{O_2} + E_{En}\ln\left(\frac{Al}{Si}\right) + \sum_{i=1}^{n} J_{En,i}X_i^l + \ln a_{MgO}^l + \ln a_{SiO_2}^l\right], \quad (3)$$

where a_i is the activity of components in the melt according to the two-lattice melt model by Nielsen with co-authors (see Frenkel et al., 1988)

The corresponding form is expressed by the remaining minals. The coefficients for variables and constants are found in equation (1) by minimizing the sum of squared differences between the calculated and experimental contents of the minals using the add-on “solution search” in the Excel program.

The optimization process, as a rule, is not one-step. Optimization results are considered satisfactory if the angular coefficient in the linear regression equation is close to 1, the free term to 0, and the residues are distributed according to the normal law. In some cases, as a result of statistical processing, linear trends on the correlation graphs of calculated and experimental values deviate significantly from the line of equal values, and there are no experiments that strongly deviate from the total array of points, while the distribution of the remaining minals is normal. In these cases an additional correction in the form of a linear equation is introduced to improve the agreement between the calculated and experimental values

$$X_m = a * X'_m + b, \quad (4)$$

where X'_m is the minal content calculated by the equation of the form (3), *a* and *b* are the coefficients in the linear trend equation of the dependence between the experimental and calculated minal contents. The optimization results are presented in Table 1.

Table 1. The values of the coefficients and constants for equations of the form (3) and (4).

	En	Fs	Wo	FeAl	AlAl	Jd	MgTi	Rdn	CrPx
A	4367.17	3672.30	4208.23	0	563.456	0	13273.2	0	0
β	18.1552	27.9113	35.9712	-2.60667	84.4695	92.7083	33.399	16.2408	-14.6675
B	-4.13849	-2.29436	-22.6408	-2.59057	3.28893	-17.669	-24.842	1.5431	-119.964
D	0.013518	0.028487	0.034226	-0.39537	0.025223	0.05696	0.052721	0.026345	-0.01207
J_{Si}	2.73761	0.51619	16.7885	-2.02774	-12.1304	12.5197	11.937	0.0000	117.0551
J_{Ti}	3.71774	0.18789	20.7392	3.74888	2.30691	23.1962	13.2311	6.7890	119.1513
J_{Al}	3.21077	0.09881	16.3215	0	4.14921	10.5077	26.2508	0.5438	126.2561
J_{Fe3+}	1.82279	-2.68149	16.0574	0	-9.99135	6.9171	7.4168	-7.4012	138.6687
J_{Fe2+}	2.81798	0	22.7085	-2.81098	3.91451	24.1806	21.9229	-1.7883	123.6371
J_{Mg}	0	-2.63958	18.2177	10.3944	-0.08665	17.6987	16.0298	-7.0613	122.5131
J_{Ca}	2.70927	0.22839	24.4795	3.67546	-2.22597	12.5589	15.9297	-1.7578	127.6212
J_{Na}	1.08326	-1.40199	22.7930	2.34936	3.46198	27.4238	10.5884	-7.8188	126.456
J_K	5.06150	-1.3922	27.5633	-7.76535	2.20319	24.6372	15.1358	-0.2909	140.271
Correction coefficients for equations of the form (4)									
a	0.82757	1	1	0.75468	1	1	1	0.9504	0.83503
b	0.136896	0	0	0.003662	0	0	0	0.000182	0.002123

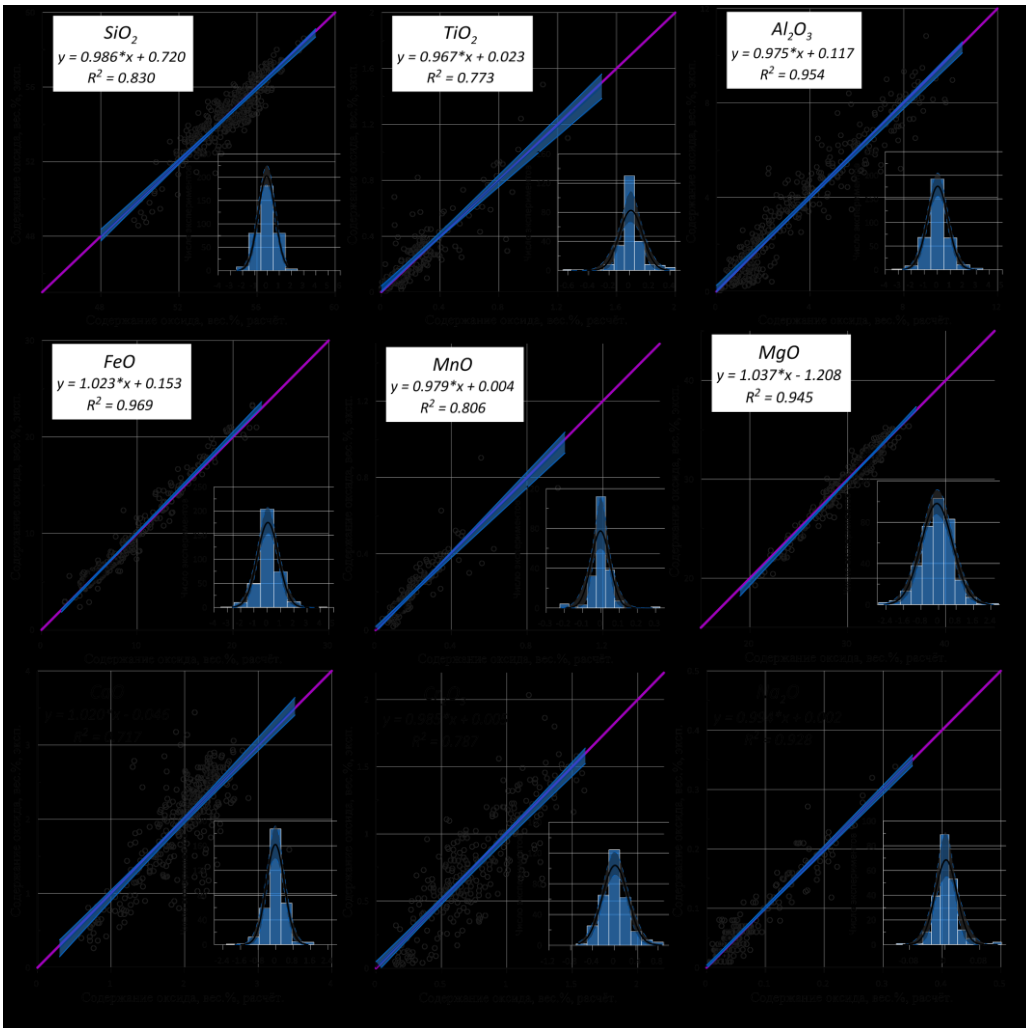

Fig. 2. Graphs of the correspondence of calculated and experimental oxide contents in orthopyroxenes and histograms of the distribution of the corresponding residues. Abscissa axis - calculation, ordinate axis - experiment, wt.%

When modeling fractionation of minerals, the extraction (or addition) of components from (in) the melt will be performed in the form of oxides. Therefore, the calculated molar contents of the minals in orthopyroxenes were converted to the weight percent of the contents of the oxides. The compositions of experimental orthopyroxenes are presented in weight percent; therefore, it is more correct to verify the calculated compositions in the same parameters. In addition, when recalculating orthopyroxenes to minals, a number of postulates were adopted, the validity of which also needs to be verified.

A comparison of the calculated and experimental compositions of orthopyroxenes is shown in Fig. 2. On the graphs in Fig. 2 and in Fig. 3, black lines - linear trends, purple lines - lines of equal values (almost coincide). On the histograms of residuals, black curves are the lines of approximation by the normal distribution. Semitransparent areas - confidence intervals at the 95% level of reliability.

One of the statistically valid criteria for the quality of compositometers is the size of the confidence interval at a given level of reliability of linear regression between experimental and calculated values. The advantage of confidence intervals for evaluating the quality of an equation, compared, for example, with standard deviations, is their visibility and the fact that the confidence interval narrows with increasing sample size. The error in predicting the content of oxides in orthopyroxenes in weight % does not exceed for: SiO_2 ±0.26, TiO_2 ±0.02, Al_2O_3 ±0.14, FeO ±0.15, MnO ±0.01, MgO ±0.28, CaO ±0.12, Na_2O ±0.01, Cr_2O_3 ±0.04. This makes it possible to model the fractionation of these elements with higher accuracy, which may be useful, for example, in geochemical thermometry procedures.

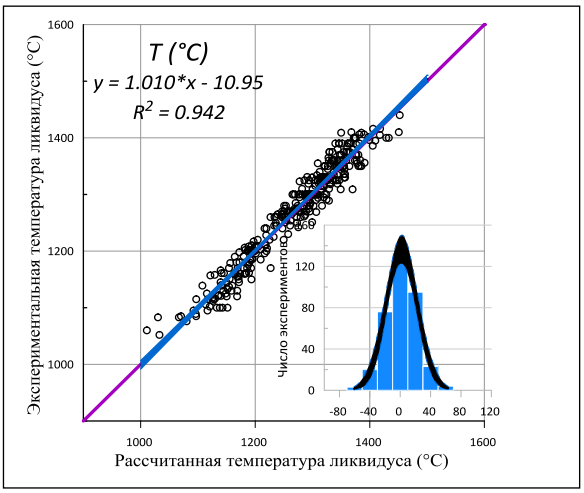

Fig.3. Correlation between experimental and calculated orthopyroxene liquidus temperatures and histogram of the distribution of temperature residues; abscissa axis - calculation, ordinate axis – experiment.

The liquidus temperatures of orthopyroxene were calculated in the CryMinal program using the "search for liquidus temperature" option. For a given melt composition, pressure, and oxygen fugacity, an iterative method is used to find the temperature at which the sum of the mole fractions of the minals in the mineral is equal to unity. This temperature is taken as the calculated liquidus temperature of the corresponding mineral. The result of these calculations is presented in Figure 3. The width of the confidence interval for estimating the temperature with a 95% probability does not exceed ±5 degrees. The line of equal values lies within the confidence corridor.

Acknowledgments. The authors are grateful to A.A. Ariskin, G.S. Barmina, and G.S.Nikolaev for the selfless efforts to create and update the INFOREX database.

References

Ariskin A. A. et al. INFOREX information retrieval system: analysis and processing of experimental data on phase equilibria in igneous rocks //Petrology. – 1997. – vol. 5. – №. 1. – p. 28-36.

Koptev-Dvornikov E.V., Bychkov D.A. Geothermometers for a wide range of compositions of basites: Mat. Conf. "Ultramafite-Mafite Complexes of Pre-Cambrian Folded Regions." Irkutsk. Izd. SB RAS, 2007. P. 178-181.

Frenkel M.Ya., Yaroshevsky A.A., Ariskin A.A., Barmina G.S., Koptev-Dvornikov E.V., Kireev B.S. Dynamics of intrachamber differentiation of basite magmas. Moscow: Nauka, 1988. 216 c.

Kotelnikov A.R., Korzhinskaya V.S., Suk N.I., Van K.V. Experimental study of zircon and hafnon solubility in silicate melts UDC 550.89

Institute of Experimental Mineralogy RAS (IEM RAS), 142432, Chernogolovka Moscow district, (kotelnik@iem.ac.ru; vkor@iem.ac.ru; sukni@iem.ac.ru)

Abstract. The solubility of zircon and hafnon in an aluminosilicate melt at temperatures of 800 and 1000°C, P 2 kbar in the presence of water or a 1M KF solution has been studied. The duration of the experiments was 5 days for 1000°C and 14 days for 800°C. In the experiments, we used synthesized by us under hydrothermal conditions zircon ($ZrSiO_4$), hafnon ($HfSiO_4$) and granite (Orlovka deposit, well 42). The influence of K_{agp} ((Na+K)/Al) on the solubility of zircon and hafnon in an aluminosilicate melt in the presence of water was established: with an increase in K_{agp} from 0.8 to 2.08, the ZrO_2 content in the glass increases on the average from 0.2 wt.% to 6.54 wt.%. For hafnon, with an increase in K_{agp} (from 1.04 to 1.86), the HfO_2 content in the glass increases on the average from 2.04 to 6.72 wt.%. It was noted that the K_{agp} of the melt has a stronger effect on the

solubility of zircon and hafnon than the temperature and the presence of fluorine.

Keywords: silicate melt, zircon, hafnon, solubility, experiment

Experimental method The solubility of zircon and hafnon in an aluminosilicate melt was experimentally studied at T=800-1000°C and P=2 kbar on a high gas pressure vessel in the presence of water or 1M KF solution. The duration of the experiments was 14 days for 800°C and 5 days for 1000°C. The experiments used zircon, hafnon synthesized under hydrothermal conditions, as well as granite (Orlovka deposit, well 42) of the following composition (wt.%): SiO_2 – 72.10%; TiO_2 – 0.01%; Al_2O_3 – 16.14%; Fe_2O_3 – 0.68%; MnO – 0.09%; CaO – 0.30%; MgO – 0.01%; Na_2O – 5.17%; K_2O – 4.28%; P_2O_5 – 0.02%; F – 0.32%; H_2O – 0.18%, which was preliminarily melted at atmospheric pressure and a temperature of 980°C. To elucidate the effect of agpaitic coefficient on the solubility of zircon and hafnon, preliminarily fused aluminosilicate glasses were prepared with different K_{agp}=(Na + K)/Al: from 0.80 to 2.5. The experiments were carried out in platinum ampoules 5x0.1x50 mm, into which about 50 mg of granite glass, 5 mg of zircon or hafnon crystals were loaded. A certain amount of water or 1 M KF solution was poured into ampoules. The ampoules were hermetically sealed and placed in a "gas" bomb for the experiment. The compositions of all samples after the experiments were determined by electron probe X-ray spectral analysis using a Tescan Vega II XMU scanning electron microscope (Tescan, Czech Republic) equipped with an INCA Energy 450 X-ray microanalysis system with energy-dispersive (INCAx-sight) and crystal diffraction (INCA wave 700) X-ray spectrometers (Oxford Instruments, England) and the INCA Energy + software platform.

Solubility of zircon and hafnon in aluminosilicate melt at T = 1000°C, P = 2 kbar Earlier, to assess the solubility of zircon in an aluminosilicate melt, we used a technique for measuring the diffusion profile of the ZrO_2 content in quenched glass from the boundary of a zircon crystal (Kotelnikov et al., 2019). Fig. 1 shows an example of the measured profile of the diffusion distribution of ZrO_2 upon dissolution of zircon in a granite melt in the presence of 1 M KF. It can be seen that at a distance of ~ 200 μm from the zircon crystal, the ZrO_2 content in the glass remains constant and then begins to decrease. This gives grounds to take these maximum values for the solubility of ZrO_2 in the melt. The solubility of hafnon in the aluminosilicate melt was studied by the similar method.

Table 1 shows the results of experiments on the solubility of zircon and hafnon in melt with different agpaiticity at T=1000°C, P=200 MPa, and Fig. 2 shows the dependence of the solubility of minerals zircon and hafnon in the aluminosilicate melt in the presence of water on agpaitic coefficient.

The dependence of the solubility of zircon in the melt in the presence of water on agpaitic coefficient is revealed: with an increase in K_{agp} from 0.8 to 2.08, the ZrO_2 content in the glass increases on average from 0.2 wt% to 6.31 wt%. The composition of the glass in wt% is as follows: Na_2O – 4.65; Al_2O_3 – 15.52; SiO_2 –65.51; K_2O – 4.55; CaO – 0.16; TiO_2 – 0.40; F – 0.95 (K_{agp} = 0.81). For hafnon, the solubility is slightly higher: with an increase in K_{agp} from 0.88 to 1.87, the HfO_2 content in glass increases on average from 0.90 wt% to 6.72 wt%. The composition of glass in this case (wt%) is as follows: Na_2O – 4.51; Al_2O_3 – 14.04;SiO_2 – 64.59; K_2O – 4.56; CaO – 0.08; TiO_2 – 0.06 (K_{agp} = 0.88).

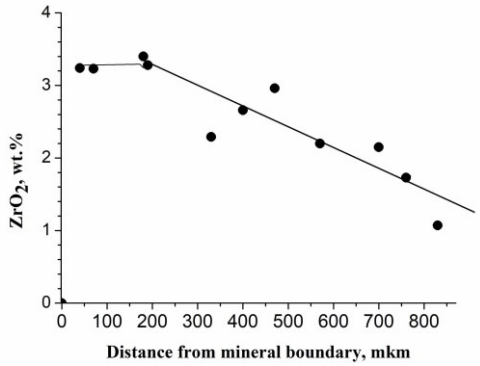

Fig. 1. An example of the measured profile of the diffusion distribution of ZrO_2 during dissolution of zircon in a granite melt with 1 M KF (K_{agp}=0.80, T=1000°C, P=2 kbar).

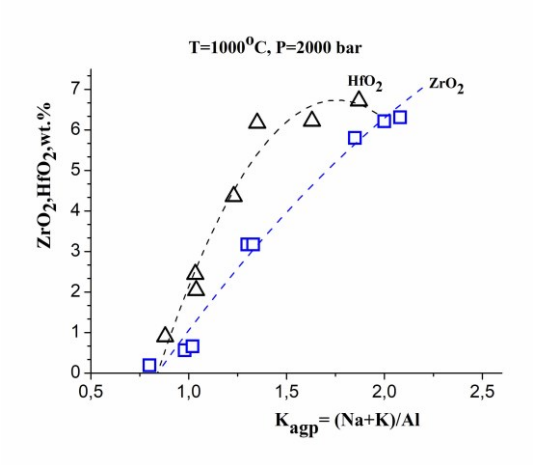

Fig. 2. Dependence of the solubility of zircon and hafnon in an aluminosilicate melt in the presence of water on agpaitic coefficient (K_{agp}=(Na + K)/Al).

Table 1. Experiments on the solubility of zircon and hafnon in melt with different agpaiticity at T=1000°C and P = 2 kbar

№ exp.	Weight, mg	Solution, mg	ZrO_2/HfO_2, wt %	K_{agp} before exp.	K_{agp} after exp.
Zrc-3	46.07 granite+4.74 Zrc	H_2O-49.48	0.19	0.81	0.80
Zrc-6	49.75 granite +5.33 Zrc	H_2O-14.90	0.56	0.95	0.98
Zrc-7	50.23 granite +5.70 Zrc	H_2O-14.94	0.66	1.09	1.02
Zrc-8	51.13 granite +5.53 Zrc	H_2O-15.10	3.172	1.19	1.3
Zrc-9	51.88 granite +6.12 Zrc	H_2O-14.94	3.17	1.51	1.33
Zrc-10	50.34 granite +5.60 Zrc	H_2O-49.57	5.80	2.0	1.85
Zrc-11	44.21 granite +4.33 Zrc	H_2O-50.15	6.21	2.3	2.0
Zrc-12	47.03 granite +5.84 Zrc	H_2O-50.13	6.31	2.5	2.08
Zrc-2	67.78 granite +5.83 Zrc	1MKF-107.71	3.43	0.81	1.55
Hfn-1	45.94 (granite +Hfn)	H_2O-52.99	0.90	0.95	0.88
Hfn-2	53.75 (granite +Hfn)	H_2O-52.99	2.04	1.09	1.038
Hfn-3	50.44 (granite +Hfn)	H_2O-52.99	2.44	1.19	1.033
Hfn-4	50.985 (granite +Hfn)	H_2O-52.99	4.36	1.25	1.23
Hfn-5	50.99 (гранит+Hfn)	H_2O-52.99	6.17	1.51	1.40
Hfn-6	50.62 granite +4.65 Hfn	H_2O-50.58	6.22	2.00	1.63
Hfn-8	46.22 granite +5.26 Hfn	H_2O-49.93	6.72	2.05	1.87
Hfn-9	48.93 granite +4.36 Hfn	1mKF-106.6	4.65	0.81	1.64

Table 2. Experiments on the solubility of zircon and hafnon in melt with different agpaiticity at T=800°C, P = 2 kbar

№ exp.	Weight, mg	Solution, mg	ZrO_2/HfO_2, wt %	K_{agp} before exp.	K_{agp} after exp.
Zrc-14	50.39 granite +3.88 Zrc	H_2O - 50.05	0.26	0.95	0.95
Zrc-15	50.50 granite +5.22 Zrc	H_2O - 50.32	0.55	1.19	1.17
Zrc-16	46.95 granite +5.38 Zrc	H_2O - 50.22	1.58	1.51	1.43
Zrc-17	52.11 granite +4.45 Zrc	H2O – 50.37	3.87	2.00	1.73
Zrc-13	51.49 granite +4.48 Zrc	1mKF-58.97	7.81	0.81	1.93
Hfn-10	51.00 granite +4.36 Hfn	H2O – 50.03	0.92	0.95	0.954
Hfn-11	50.53 granite +4.27 Hfn	H2O – 50.53	2.65	1.19	1.14
Hfn-12	52.42 granite +4.00 Hfn	H2O – 49.93	4.86	1.51	1.375
Hfn-13	51.12 granite +4.16 Hfn	H2O – 49.85	9.96	2.00	1.84
Hfn-14	50.77 granite +4.00 Hfn	H2O – 49.78	4.50	2.50	1.785

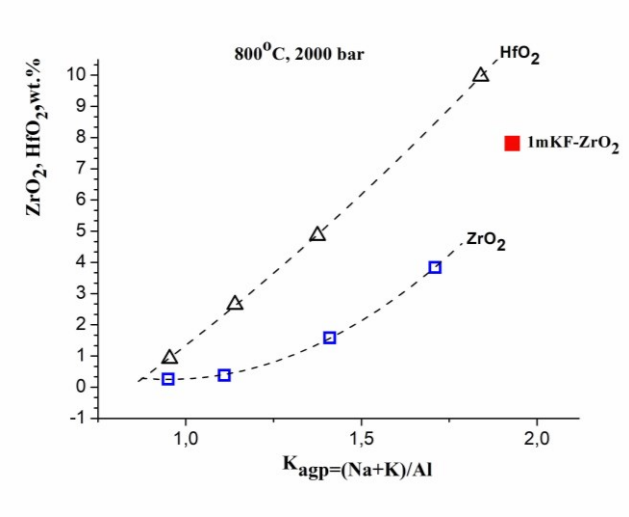

Fig. 3. Dependence of the solubility of zircon and hafnon in an aluminosilicate melt in the presence of water on agpaitic coefficient (K_{agp}=(Na + K)/Al).

In experiments with a solution of 1M KF, the composition of glass upon dissolution of zircon changed towards an increase in alkalinity and fluorine content (wt %): Na_2O – 3.95; Al_2O_3 – 11.51; SiO_2 – 57.05; K_2O – 10.82; MnO – 0.50; F – 2.56 (K_{agp}=1.58). The solubility of ZrO_2 in glass is 3.43 wt% under these conditions. The agpaitic coefficient doubled: from 0.81 to 1.58, which led to an increase in the solubility of ZrO_2 by at least 10 times. In experiments on the solubility of hafnon, the composition of the glass changed towards an increase in alkalinity and fluorine content (wt%): Na_2O – 3.19%; Al_2O_3 –11.82%; SiO_2 – 57.11%; K_2O – 13.04%; MnO – 0.14%; F – 2.24% (K_{agp} =1.64). The solubility of HfO_2 in glass is 4.65 wt% under these conditions. The agpaitic coefficient doubled: from 0.81 to 1.64, which led to an increase in the solubility of HfO_2 from 0.9 to 4.65 wt%.

Solubility of zircon and hafnon in aluminosilicate melt at T = 800°C, P = 2 kbar

Table 2 shows the results of experiments on the solubility of zircon and hafnon in a melt with different agpaiticity at T=800°C, P=2 kbar, and Fig. 3 shows the dependence of the solubility of minerals zircon and hafnon in the presence of water on agpaiticity. The solubility of zircon in presence of 1M KF solution is also shown, which is 7.81 wt%, while the agpaitic coefficient increases from 0.81 to 1.93. The solubility of hafnon for granite with agpaitic coefficient of 0.81 is an order of magnitude higher than the solubility of zircon. And with an increase in agpaiticity (K_{agp}=(Na + K)/Al), it grows

to 10 wt% (K_{agp} = 1.84), which is higher than at the same agpaiticity for 1000°C (6.72 wt%).

As a result of the studies carried out on the solubility of zircon and hafnon in aluminosilicate melt, it was found that the agpaiticity of the melt has a stronger effect on the solubility of these minerals than the temperature and the presence of fluorine.

This work was supported by the AAAA-A18-118020590151-3 program.

Reference

Kotelnikov A.R., Korzhinskaya V.S., Suk N.I., Van K.V., Virus A.A. Experimental study of zircon and loparite solubility in silicate melts. Experiment in GeoSciences. 2019. V. 25. N 1. P. 138-140.

Kotelnikov A.R.[1], Suk N.I.[1] Damdinov B.B.[2], Damdinova L.B.[2], Khubanov V.B.[2] Experimental studies of phenakite solubility in silicate melts UDC 550.89

[1]Institute of Experimental Mineralogy RAS (IEM RAS), 142432, Chernogolovka, Moscow district, Russia (kotelnik@iem.ac.ru; sukni@iem.ac.ru); [2]Institute of geology SD RAS (IG SD RAS), 670047, Ulan-Ude, Russia (damdinov@mail.ru)

Abstract. The solubility of phenakite in aluminosilicate melts of various compositions was experimentally studied at T=1000°C and P=1 kbar in dry conditions and in the presence of 10 wt.% H_2O. The experiments were carried out on a high gas pressure vessel. The duration of the experiments was 5 days. The initial material was pre-fused glass of granite composition with different agpaiticity (1-1.5), as well as natural phenakite. The composition of the samples after the experiments was determined by the method of electron probe x-ray spectral analysis, the beryllium content was determined by laser ablation. It was found that the solubility of phenakite depends on the composition of the aluminosilicate melt, increasing with increasing agpaiticity ((Na + K)/Al).

Keywords: silicate melt, phenakite, solubility, experiment

Beryllium is one of the most important rare elements (such as Nb, Ta, Mo, W, Sn, etc.) required for the high-tech industry (nuclear power, metallurgy, mechanical engineering). Geochemically, beryllium is associated with granites, in particular with varieties of lithium-fluoride granites, alkaline granites and pegmatites. Problems of the genesis of beryllium minerals in the evolution of fluid-magmatic systems attract the attention of many researchers. However, experimental data on the solubility of beryllium in granite melts are almost completely absent. This is most likely due to analytical problems, as well as the high toxicity of beryllium compounds. Nevertheless, the development of modern methods of analysis and experimental research methods allowed us to start studying the solubility of phenakite (Be_2SiO_4) in granite melts with different values of the agpaitic coefficients (K_{agp}=(Na + K)/Al).

The solubility of phenakite in aluminosilicate melts of various compositions was experimentally studied at T=1000°C and P=1 kbar in dry conditions and in the presence of water. The experiments were carried out on a high gas pressure vessel. Preliminarily melted glasses of granite composition with different agpaiticity (1, 1.2, 1.5), as well as natural phenakite were used as the starting material. The experiments were carried out in sealed platinum ampoules with a diameter of 3 mm, where a sample was placed (70 mg of granite glass + 14 mg of phenakite) and, if necessary, water was poured (7 μL). The duration of the experiments was 5 days, and then isobaric quenching was carried out. The compositions of the samples obtained were determined on a Tescan Vega II XMU scanning electron microscope (Czech Republic) equipped with energy dispersive (INCAx-sight) and crystal diffraction (INCA wave) X-ray spectrometers (England, Oxford). The program of qualitative and quantitative analysis INCA Energy 450 was used. The content of beryllium was determined by laser ablation in combination with ICP MS.

As a result of experiments, glass with phenakite crystals was obtained. The composition of the glass was determined near the crystals and is presented in Table. 1. Analyzes in Table 1 are reduced to 100 wt. %.

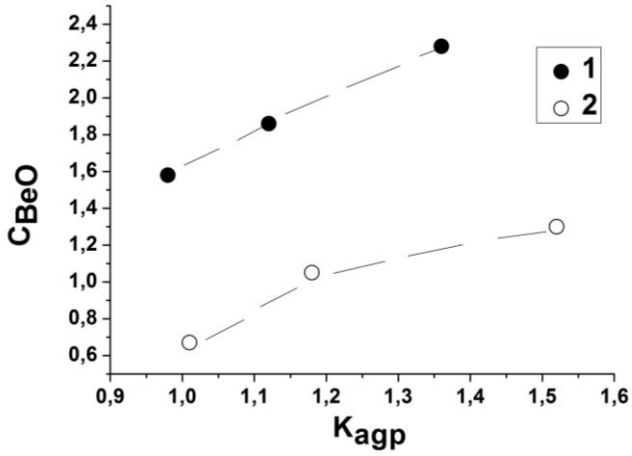

Fig. 1. Dependence of the BeO content (wt%) on the agpaiticity of the aluminosilicate melt (Na+K)/Al. 1 – experiments carried out in the presence of water fluid, 2 – experiments carried out under dry conditions.

It was found that the solubility of phenakite depends on the composition of the aluminosilicate melt (Fig. 1), increasing with an increase in its agpaitic coefficient ((Na+K)/Al). At the same time, the agpaitic coefficient in water-containing systems slightly decreases compared to the initial value, which can be explained by the partial dissolution of alkalis in the fluid. The data obtained show that the

solubility of phenakite in glass in the presence of water fluid is higher than in dry conditions. Based on the data obtained, the linear dependences of the solubility of phenakite on K_{agp} were calculated:

C_{BeO} (%)=-0.206 + 1.832*(K_{agp}); s_x=0.01; E_x=0.02; ("Watered" conditions)
C_{BeO} (%) = -0.443 + 1.174*(K_{agp}); s_x=0.07; E_x=0.11; ("Dry" conditions).

In water-containing melts, the solubility of BeO is approximately two times higher than in dry ones. In addition, the dependence of the solubility on the alkalinity of the aluminosilicate melt in water-containing melts is ~ 1.6 times higher than in dry ones. This fact testifies in favor of the model of beryllium concentration in residual alkaline water-containing melts. These melts are formed during the phenomena of heterogenization in fluid-magmatic systems associated with decompression during the evolution of granite melts.

Table 1. Compositions of experimental glasses obtained at T=1000°C and P=1 kbar

	In the presence of H_2O			Dry conditions		
№	7286	7287	7288	7289	7290	7291
SiO_2	72.32	71.31	71.17	71.91	70.63	69.80
Al_2O_3	14.75	13.80	12.96	15.31	14.88	13.23
Na_2O	5.50	5.68	6.48	5.96	6.91	7.72
K_2O	5.06	5.63	6.50	5.23	5.74	6.84
CaO	0.47	1.52	0.42	0.57	0.36	0.62
FeO	0.32	0.20	0.18	0.35	0.42	0.48
BeO	1.58	1.86	2.28	0.67	1.05	1.30
Sum	100.00	100.00	99.99	100.00	99.99	99.99
K_{agp}	0.98	1.12	1.36	1.01	1.18	1.52

(compositions are reduced to 100 wt.%).

This work was supported by the AAAA-A18-118020590151-3 program.

Novikova A.S., Alferyeva Ya. O., Gramenitskiy E.N. Phase relationship modelling in syrostan massive near-contact zone by 1 kbar and 900 and 850 °C. UDC 552.113

Lomonosov State University, Geological Dep., Moscow (novikova-a-s@andex.ru)

Abstract. Diorite-tonalite-granite series from Syrostan massive were melted at the temperature 900°C and 850° C and pressure 1 kBar. Host rocks partial melting in research has shown that paragenetic mineral assemblage differs from nature ones. Newborn minerals composition in all rocks shifts towards SiO_2-depleted minerals.

Keywords: *Syrostan massif; granite and dolerite melting; experimental study; phase relationships; liquid phase relationships; variation in phase composition; granitization; magmatic replacement*

One of the largest intrusions in Syrostan-Turgoyak gabbro-diorite-granite series is Syrostan massif. Except Syrostan massif, it includes Turgoyak, Valezhnegorsk and Atlian intrusions. (Fershtater et al, 2000). All of them have the same geological structure and mineralogical composition and are situated in the Main Uralian Fault, westwards of granite zone in Uyta and Urenginsk metamorphic series. (Makagonov et al.,2015)

Due to previous works Syrostan has complex concentric zonal structure. Mostly it contains Bt-granites, located in the central part of the massif. In northern and south-western border it consists of granodiorites, and in north-eastern, eastern and southern border it contains vein granites and plagiogranites, which form 3 km width zone. (Makagonov et al.,2015).

Approximate age for Syrostan rocks according to Pb-Pb dating method is 327± 4 million years for granites and 333±3 million years for gabbro and granodiorites. (Montero et al,2000)

These data show that between mafic and intermediate subalkaline xenolites in Bt-granites, situated in eastern part of Syrostan, in contact area there occur intermediate rocks, such as diorites, Bt-Amph- tonalite, Amph-Bt – tonalite, which repeat xenolite contours. (fig.1, fig.2.)

Detail rock exploration shows relationship between mineralogical and chemical phase compound. All intermediate rocks have the same mineral composition, but different mineral quantitative ratio. (tab.1). From melanocratic to leicocratic rocks Ampibole, Mica and Plagioclase content decreases and Quatz increases. Also (fig.3) SiO_2, Na_2O and K_2O content from gabbro to granite raises and TiO_2, MgO and Fe_2O_3 content gets lower. Thus there is uneven magnesiality distribution. General trend goes towards magnesiality decrease by SiO_2 raising, but in the middle part in Amph-Bt-tonalite there is Mg# minimum.

With SiO_2 increasing from diorite to Amph-Bt-tonalite, amphibole composition changes sequentially from edenite-pargasite to tremolite, and in plagioclase composition An minal content naturally decreases.

Fig.1. Tonalite and diorite xenolites in Bt-granite.

Fig.2. Bt-granite and diorite xenolite contact area.

1 – diorite, 2 – Bt-Amph –tonalite, 3 – Amph-Bt-tonalite, 4 – Bt-granite.

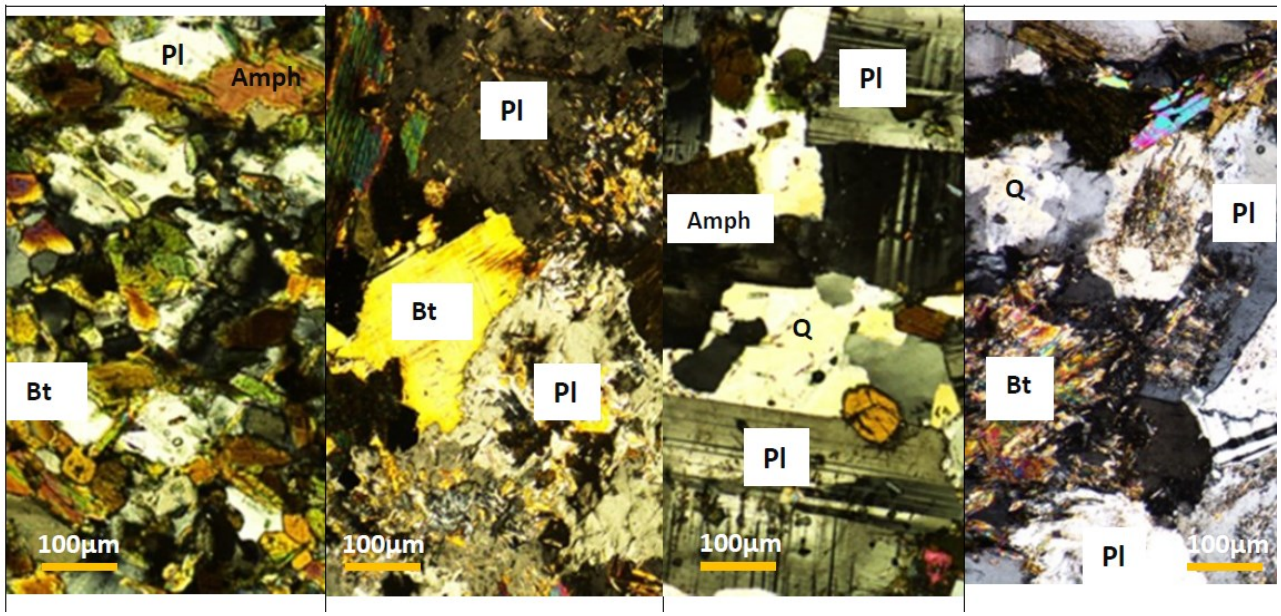

Diorite | Bt-Amph tonalite | Amph-Bt tonalite | Bt-granite

Amph – amphibole; Bt-biotite; Pl-plagioclase; Q – quartz;

Fig.3 Thin sections of initial Syrostan contact area rocks.

To estimate the interaction mechanism between granite melt and basic rocks, a few experiments have been conducted by different temperature variation and the same pressure and water amount (T1=900°C and T2=850°C, p =1 kBar, c H2O = 10 per cent from weighed portion) with diorite, Bt-Amph- и Amph-Bt – tonalite, Bt- granite . All experiments have being held on hydrothermal high-pressure plant in Chernogolovka. It lasted in the first experiment for 3 days, and in the second – for 5 days.

Rocks heating results in partial samples melting and effective mineral transformation. Partial diorite melting at 900, and 850 °C has shown, that Bt was melted, Pl –was partly melted. (Tab.1)

In Bt-Amph-tonalite at 900°C stable phases are Pl, Amph, Ol. Cooling system at 50°C results in changing phase stability. Newborn minerals for them are Q, Amph, Pl. (Tab.1)

At 900 °C Amph-Bt – tonalite is also in part-melting condition. Q and Bt disappear and Ol, Amph and Pl become newborn phases. At 850 °C in rocks solution of Pl crystals and forming of melt (by 15%), Amph and Pl take place. (Tab.1)

In the next rock – Bt-granite under 900 °C occur Amph and Pl and Q dissolution. Kfs, Q, Amph and Pl become stable with temperature decrease. (Tab.1) All new data have shown that paragenetic mineral assemblage in experiments differs from nature ones. Newborn minerals composition in all rocks shifts towards SiO_2-depleted minerals.

Such minerals, as Ol and Px crystallize in new rock composition, that have not been met in nature samples. They were formed by partial melting of basic rocks, such as Bt-Amph-tonalite and Amph-Bt-tonalite.

Ol was formed in Bt-Amph-tonalite at 900 ℃, and Px appeared in Q-Act-shale at 850 and 900 ℃. Their formation is a result of partial rock melting and crystallization of SiO2-depleted phases.

Generated Pl crystals in all rocks differ from each other in composition under high temperature. Pl composition is displaced in all melanocratic and in granite samples about nature samples towards A minal at 900 ℃, and 850 ºC Pl is identical with original. In leicocratic rocks new equilibrium phases are Pl and Kfs, which contrast with the nature ones by high Ort minal content in andesine and Ab minal in sanidine.

Tab.1 Phase relationship comparison in experimental products and initial contact area rocks of Syrostan massif.

	Bt-diorite				**Bt-Amph-tonalite**					
Initial samples	L,%	Pl,%	Amph,%	Bt,%	L,%	Pl,%	Amph,%	Bt,%	Q,%	Ol,%
	-	50	30	20	-	55	15	10	20	-
T=900 C	15	45	40	-	45	40	15	-	-	10
T=850 C	10	60	30	-	35	40	15	-	10	-

	Amph-Bt-tonalite						**Bt-granite**					
Initial samples	L,%	Pl,%	Amph,%	Bt,%	Q,%	Ol,%	L,%	Pl,%	Q,%	Bt,%	Kfs,%	Amph,%
	-	50	10	20	20	-	-	30	40	10	20	
T=900 C	25	40	25	-	-	10	65	10	25	-	-	5
T=850 C	15	70	10	5	-	-	70	10	20	-	-	5

Conclusions. All rocks have reached liquidus point at experimental parameters. New generated mineral composition in all rocks shifts towards SiO_2-depleted minerals. Pl composition is displaced towards increasing role of An minal and Amph changes from tremolite to edenite-pergasite in experiments.

In experimental samples new mineral basic phases were generated: olivine in tonalites and amphibole in Bt-granite. Partly melted rock composition in experiment is richer in SiO_2 then bulk rock composition.

These data have demonstrated the lack of naturally formed mineral association in experimental samples. It can be explained by magmatic replacement, but this hypothesis needs an experimental study, which would show diffusion or infiltration interaction of granite melt and country rocks.

References

Makagonov E.P., Muftahov V.A. Rare-earth and rare-metal mineralization in late granite of Syrostan massif (Southern Urals). LITHOSPHERE (Russia). 2015;(2):121-132. (In Russian.)

Montero P., Bea F., Gerdes A., et al., Tectonophysics 317, 93–108 (2000).

Fershtater G. B., Shagalov E. S., Bea F., and Montero P. V., in Igneous and Metamorphic units of the Urals and Their Metallgenies (IGiG UrO RAN, Yekaterinburg, 2000) [in Russian].

Romanova E.S., Koptev-Dvornikov E.V., Bychkov D.A. Pigeonite liquidus thermobarometer for a range of melts compositions from magnesial basites to dacites. UDC 552.111: 550.41

Lomonosov Moscow State University, Department of Geology, Moscow (katrin.s.romanova@gmail).

Abstract. To date, thermodynamic, semi-empirical and empirical models have been developed to predict the crystallization of olivine, plagioclase, augite, orthopyroxene and ore minerals (sulfides, chromium spinels, magnetite and ilmenite). In order to model the equilibrium in basite - hyperbasite systems, it remains to derive a thermobarometer-compositometer for pigeonite.

From the Lepr 3.0 and INFOREX databases, 227 "dry" quenching experiments (51 of which are high pressure up to 30 kbar) were extracted, characterizing the compositions of coexisting pigeonites and melts. As a result of this work, a system of equations of the pigeonite thermobarometer, describing the equilibrium with the silicate melt in a wide range of compositions, temperatures, pressures and oxygen fugacity with high accuracy was developed.

The liquidus thermobarometers obtained for the first time allow to predict not only the main oxides, but also secondary components (TiO_2, Al_2O_3, MnO, Na_2O, Cr_2O_3) in the composition of pigeonites.

Keywords: pigeonite, silicate melt, equilibrium, equation, thermobarometer, modeling.

By now, our scientific group has developed a complex of thermobarometer-composite meters, which allows us to predict the crystallization of olivine, plagioclase, augite, orthopyroxene and ore minerals (sulfides, chromspinelides, magnetite and ilmenite). In order to model the equilibrium in basite-hyrbasite systems, it remains to derive a thermobarometer-composite for pigeonite.

Lepr 3.0 (Hirshmann M.M., et al., 2008) and INFOREX (Ariskin et al., 1992) databases were used to create the sample. However, for our research experiments in which pyroxene is a pigeonite by its author's definition were not enough, and it was decided to collect data on all pyroxenes. For our queries in Lepr 3.0 and INFOREX databases 5 samples were compiled and those experiments in which the content of the wollastonite minal in the pyroxene was in the range from 5% to 20% were selected, because according to the international classification (Morimoto, 1988) such pyroxenes belong to the pigeonite.

The polyhedron of experimental melt compositions in the concentration coordinates of melt oxides for the final sample of 227 experimental values is characterized by the following values (in weight percentages): SiO_2 from 40,27 to 68,10, TiO_2 from 0 to 10,7, Al_2O_3 from 1 to 17,8, FeO* from 0,34 to 28,3 (FeO* – all iron, converted to FeO), MnO from 0 to 0,56, MgO from 1 to 16,1, CaO from 2,03 to 15,68, Na_2O from 0 to 4,34, K_2O from 0 to 4,28, Cr_2O_3 from 0 to 1,11.

The range of intensive parameters is characterized by: temperature from 960 to 1400°C, pressure from 1 bar to 30 kbar, oxygen fugacity from -14.5 to -4.95.

Having reviewed a number of approaches to take the system composition into account when calculating the equilibrium constant, E.V. Koptev-Dvornikov and D.A. Bychkov (Koptev-Dvornikov, Bychkov, 2007) stopped at the following kind of equation:

$$\ln K_m^j = \frac{A_m^j + \beta_m^j P}{T} + B_m^j + C_m^j T + D_m^j \lg fO_2 + E_m^j \ln\left(\frac{\mathrm{Al}}{\mathrm{Si}}\right) + F_m^j W + \sum_{i=1}^{n} J_{m,i}^j X_i^l, \quad (1),$$

where K_m^j – constant of reaction of formation of minal **m** of crystal phase **j**; ***P*** – pressure in kbar; ***T*** – absolute temperature; $\boldsymbol{fO_2}$ – oxygen fugacity in bars, $\boldsymbol{W}=\ln((Na+K)Al/Si^2)$, $\boldsymbol{X_i}$ – molar fraction of ***i***-th component of melt, ***n*** - number of considered components. Parameters Al/Si and *W* (calculated using atomic quantities of elements) are proposed (Ariskin, Barmina, 2000), *A, β, D, E, F, J* - coefficients with corresponding variables, *B* - constant.

The calculation of these coefficients is based on the principle of using multidimensional statistical methods.

Traditionally, the composition of the pigeonite is recalculated into three minals - ferrosilite, enstatite and wollastonite. However, both in natural samples and in experimental pigeonites, microprobe analysis detects the presence of TiO_2, Al_2O_3, MnO, Na_2O, Cr_2O_3 in quantities reaching the first percent. In this regard, we recalculated the chemical compositions of the pigeonites by 9 minals. – enstatite $MgSiO_3$ (En), ferrosilite $FeSiO_3$ (Fs), wollastonite $CaSiO_3$ (Wo), feral $FeAlO_3$ (FeAl), alal $AlAlO_3$ (AlAl), jadeite $Na_{0.5}Al_{0.5}SiO_3$ (Jd), magti $MgTiO_3$ (MgTi), rhodonite $MnSiO_3$ (Rdn), chrompyroxene $CrSiO_3$ (CrPx).

The formation of the above mentioned minals from the melt is described by the following heterophase reactions:

$MgO^l + SiO_2^l = MgSiO_3$	**(En)**
$FeO^l + SiO_2^l = FeSiO_3$	**(Fs)**
$CaO^l + SiO_2^l = CaSiO_3$	**(Wo)**
$FeO^l_{1,5} + AlO^l_{1,5} = FeAlO_3$	**(FeAl)**
$AlO^l_{1,5} + AlO^l_{1,5} = AlAlO_3$	**(AlAl)**
$0{,}5NaO^l_{0,5}+0{,}5AlO^l_{1,5}+SiO^l_2=$ $=Na_{0,5}Al_{0,5}SiO_3$	**(Jd)**
$MgO^l + TiO^l_2 = MgTiO_3$	**(MgTi)**
$MnO^l + SiO^l_2 = MnSiO_3$	**(Rdn)**
$CrO^l + SiO_2^l = CrSiO_3$	**(CrPx)**

(2)

From the type of equation (1) and reactions (2), expressions for calculating the contents of pigeonite minals in a mineral are as follows. Example for an enstatite minal (3)

$$X_{En} = \exp\left[\frac{(A_{En} + \beta_{En} P)}{T} + B_{En} + D_{En} \lg f_{O_2} + E_{En} \ln\left(\frac{Al}{Si}\right) + \sum_{i=1}^{n} J_{En,i} X_i^l + \ln a_{MgO}^l + \ln a_{SiO_2}^l\right] \quad (3),$$

where a_i – activities of the initial components in the melt according to the two-grid model of silicate liquid by Nielsen's with the coauthors (see Frankel et al., 1988).

The corresponding form has expressions for other minals. Finding the coefficients for variables and constants in equation (1) is done by minimizing the sum of squares of difference between the calculated and experimental contents of the minals using the superstructure "solution search" in Excel program. As a rule, the optimization process is not one-act. Optimization results are considered satisfactory if the angular coefficient in the linear regression equation is close to 1, the free term to 0, and the residues are distributed according to normal law. In a number of cases, as a result of statistical processing, linear trends on the correlation graphs of calculated and experimental values deviate significantly from the line of equal values, and there are no experiments that deviate strongly from the general array of points, while the distribution of residues of minals is normal. In these cases, to improve the coordination between the calculated and experimental values, an additional

correction in the form of a linear equation is introduced.

$$X_m = a * X'_m + b \quad (4)$$

where X'_m – minal content calculated using equation of species (1), a and b - coefficients in the linear trend equation of dependence between experimental and calculated minal content.

Table 1. The values of the coefficients and constants for equations of the form (3) and (4).

	En	Fs	Wo	FeAl	AlAl	Jd	MgTi	Rdn	CrPx
A	3944,89	5308,95	4406,57	0,00	0,00	0,00	4476,17	1686,04	1360,62
β	9,12043	12,7683	17,1025	49,9376	42,2311	2,17220	36,2871	0,58530	100,814
B	-3,60337	-3,96222	-13,5923	-37,7525	4,74113	-5,92879	-12,2971	-3,93131	-9,73007
D	0,00820	-0,00040	0,06389	-0,26984	0,05965	0,35764	-0,08845	0,01947	0,06096
Si	2,29407	0,29470	8,57519	27,4473	-16,8725	0,00	6,66597	3,66614	10,7258
Ti	3,24824	-0,11609	11,0247	15,7400	2,03030	52,6683	8,86163	2,56450	4,77123
Al	3,38778	1,15253	7,65075	42,8000	2,33822	21,6093	10,8942	5,13237	14,2870
Fe^{3+}	1,28241	4,46940	5,91665	0,0000	-1,15065	-21,6609	14,6914	2,41978	36,4881
Fe^{2+}	2,30856	0,0000	11,2863	46,7511	6,73871	16,2505	12,7481	3,98156	7,72348
Mg	0,00	0,25612	4,61931	46,8569	5,31002	15,8802	0,00	-0,07331	-1,37603
Ca	1,90973	-1,01480	22,9558	48,4737	2,07805	-16,1432	8,88527	1,24319	17,9263
Na	0,83271	-1,45977	14,8996	49,7703	10,7849	0,00	4,93616	0,93810	5,47117
K	4,78755	1,93446	25,3723	81,0854	53,4872	35,4488	13,2848	1,99942	-46,5175
Correction factors for equations of the form (4)									
q2	0,88923	1,000	1,000	0,87375	0,97804	0,95270	0,93869	0,90112	0,92653
q3	0,07206	0,00000	0,00000	0,00170	0,00054	0,00072	0,00055	0,00072	0,00082

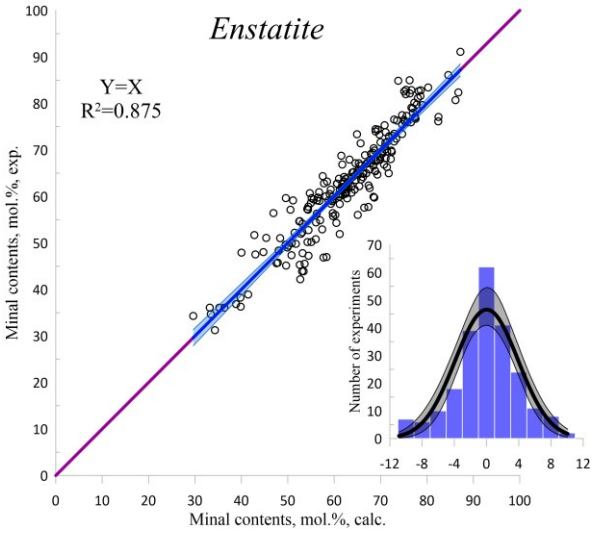

Fig.1.

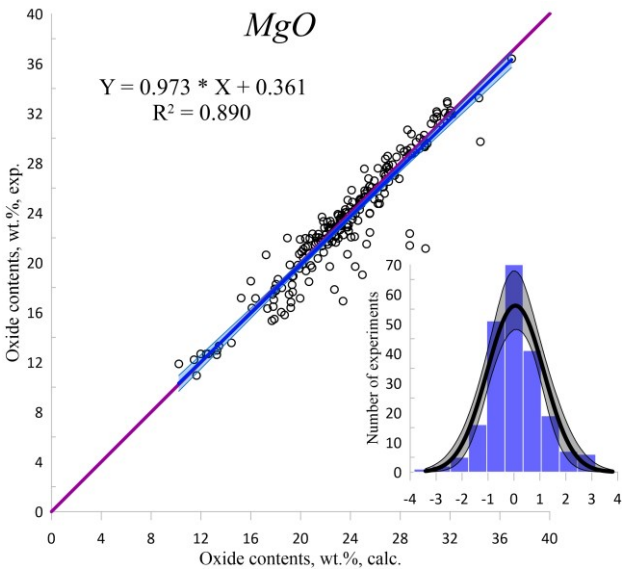

Fig.2.

Figure 1: Graph of correspondence between the calculated and experimental contents of enstatites in pigeonites. Blue line - linear trend, purple line - line of equal values (practically coincide). On the histogram black curve - line of approximation by normal distribution. Semi-transparent areas - confidence intervals of approximations at 95% level of reliability.

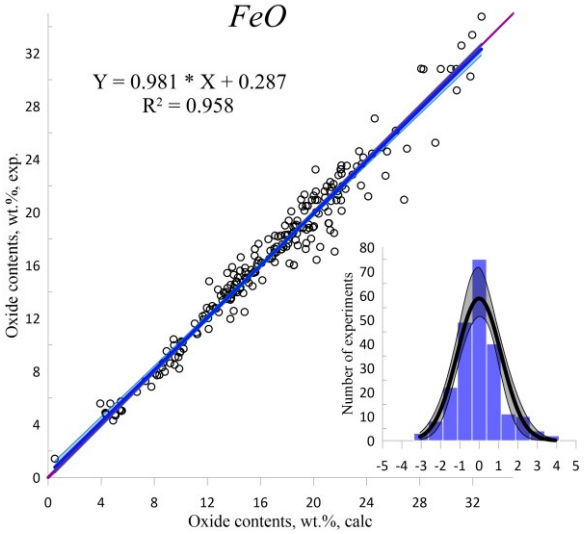

Fig.3.

Figures 2 to 3. Graphs of correspondence between the calculated and experimental contents of oxides in pigeonites in equilibrium with melts (227 experiments in the sample) and histograms of distribution of the corresponding residues. See Fig. 1 for symbols.

As an example of the nature of the correlations between the calculated and experimental content of the minerals, we give a graph for the main minal - enstatite (Fig. 1).

The purpose of development of liquidus thermobarometers is not in prediction of compositions of solid phases in the form of molar fractions of minals, but in prediction of their compositions in the form of weight percent of oxides, because when modeling the fractionation of minerals it is in the form of oxides will be carried out extraction (or addition) of components from (in) the melt. The composition of experimental pigeonites is presented in weight percent, so verification of the calculated compositions must be performed in the same parameters. In addition, when calculating the pigeonites for minals, a number of postulates have been adopted, whose fairness also needs to be verified.

Thus, the contents of the calculated minals were recalculated by weight percent of oxide contents. The result is shown in Figures 2-3.

According to histograms in Figures 2-3, the distribution of residues is close to normal. This is also confirmed by the criterion of consent. Despite the relative friability of point clouds in some charts, thanks to the large sample size, the width of trust corridors is small, and lines of equal values lie within these narrow corridors (Figures 2-3).

Another important quality characteristic of thermobarometers is the average value of differences between the experimental and calculated concentrations of components in minerals. The proximity of this characteristic to zero means that there is no offset of the estimated value. The average values for the oxides in our sample are less than 0.08% for main components and 0.03% for small components.

In the temperature range from 960°C to 1400°C with a 95% probability the calculated value of the pigeonite liquidus temperature differs from the unknown true one by a value not exceeding 4.9°C.

References

Ariskin A.A., Meshalkin S.S., Almeev R.R., Barmina G.S., Nikolaev G.S. INFOREX information retrieval system: analysis and processing of experimental data on phase equilibria of igneous rocks // Petrology. - 1997. - T. 5, No. 1. P. 32–41.

Ariskin AA, Barmina G. S. Modeling of phase equilibria during crystallization of basaltic magmas. - M.: Science, MAIK "Science / Interperiodica", 2000. - 363 p.

Frenkel M.Ya., Yaroshevsky A.A., Ariskin A.A., Barmina G.S., KoptevDvornikov E.V., Kireev B.S. Dynamics of intracameral differentiation of basic magmas. M .: Nauka, 1988.216 s.Ariskin A.A., Bouadze K.V., Meshalkin S.S., Tsekhonya T.I. INFOREX: A database on experimental studies of phase relations in silicate systems // Amer. Mineral. 1992. Vol.77.p.668-669

Hirschmann MM, Ghiorso MS, Davis FA, Gordon SM, Mukherjee S, Grove TL, Krawczynski M, Medard E, Till CB (2008) Library of experimental phase relations: a database and web portal for experimental magmatic phase equilibria data. Geochem Geophys Geosyst 9, Q03011, doi:10.1029/2007GC001894

Koptev-Dvornikov EV, Bychkov D.A. Geothermometers for a wide range of mafic compositions // Materials of the international conference “Ultrabasite-mafic complexes of folded areas”. Irkutsk: Publishing House of the SB RAS, 2007. P. 178–181.

Morimoto N. Nomenclature of pyroxenes //Mineralogy and Petrology. – 1988. – T. 39. – №. 1. – C. 55-76.

Seliutina N.E.[1,2], Safonov O.G.[2,1], Varlamov D.A.[2] Petrological and experimental study of syenitization of tonalite gneisses exemplified by the midiapala massif, limpopo complex, South Africa. UDC 552.11

[1]Lomonosov Moscow State University, Department of Geology, Moscow; [2] D.S. Korzhinskii Institute of Experimental Mineralogy RAS, Chernogolovka (seliutinane@gmail.com)

Abstract. The paper describes the process of syenitization of tonalite-trondhemite-granodiorite (TTG) gneisses exemplified by the rocks of the Madiapala syenite massif, Limpopo Complex, South Africa. Petrological and geochemical study of the Madiapala syenites and syenitized gneisses indicated that the rocks of this massif were formed as a result of interaction of the Alldays TTG gneisses with complex CO_2-H_2O-salt fluids at temperatures of 800-850°C and pressures of 6-9 kbar. An experimental study confirms the possibility of the formation of the assemblage clinopyroxene + titanite ± K-feldspar coexisting with the syenite melt due to reactions of Ti-bearing biotite with quartz and plagioclase at 850°C and 6 kbar.

Keywords: syenites; TTG gneisses; fluids; Limpopo complex

The Midiapala syenite massif is located in the western part of the Central Zone (CZ) of the Limpopo Complex (South Africa) within the host Alldays tonalite-trondhjemite-granodiorite (TTG) gneisses of an age of 2610-2650 Ma. According to the geochronological data obtained by the SHRIMP method (Rigby et al., 2011), the age of the syenites is 2010.3 ± 4.5 Ma. This age corresponds to the latest Paleoproterozoic event (D3/M3) in the Central Zone, which was characterized by active fluid penetration along regional and local shear-zones. Using the pseudosection method (THERMOCALC software), Rigby et al. (2008) established the maximum PT parameters of 6 kbar and 770°C for syenites. These data were interpreted as conditions of metamorphism of pre-existing syenites during the D3/M3 stage. A alternative model of the formation of syenites in the TTG gneisses (Safonov, Aranovich, 2014; Safonov et

al., 2014) is based on experiments on the interaction of biotite-amphibole tonalite gneiss with fluids H_2O-CO_2-(K, Na)Cl at 750 and 800°C and 5.5 kbar (Safonov et al., 2012, 2014). These experiments demonstrated that the leading factor for formation of the syenite assemblages from tonalite gneiss is an increase of alkali activity in a fluid. Thus, the syenite rocks could have been a product of syenitization of tonalite gneisses due to the effect of salt-rich aqueous-carbonic fluids.

Geochemical data (ICP-MS, ICP-AES) for the syenite rocks, syenitized gneisses and host TTG gneisses of the Madiapala complex distinguished two types of the syenite rocks (syenites and syenodiorites), confirmed the crustal nature of the syenite rocks and their close genetic relationship to the country tonalite gneisses. The REE spectra for the syenites indicate an extensive crystallization differentiation within the massif.

The earliest assemblage of the syenite rocks is potassium feldspar + clinopyroxene + titanite ± apatite and the later assemblage is amphibole + albite. In order to estimate the conditions for formation of the primary assemblage, the P-T pseudosections and isopleths of Mg# and Na content in clinopyroxene in association with alkali fieldspar and titanite were constructed using the PERPLE_X software (version 6.7.7 for Windows) (Connolly, 2005) for the bulk compositions of the syenites. They revealed that the primary magmatic syenite assemblage corresponded to a temperature range of 800-850°C and pressures of 6-9 kbar. Estimates on the potassium activity effect on the Alldays gneisses by calculating the $\lg(aH_2O)$ - $\lg(aK_2O)$ pseudosections showed that transformation of the gneiss into syenite is possible at constant P and T due to an increase of K_2O activity.

In order to reproduce the syenite assemblage, experiments on the interaction of a biotite tonalite gneiss (Alldays gneiss) with a H_2O-CO_2-(K, Na)Cl fluid were performed at 850°C and 6 kbar using gas pressure vessel with internal heating. The experiments were set for 10 days. The initial starting materials were solid cylindrical fragments of the Alldays gneiss and fluid mixture of oxalic acid with KCl and NaCl. The experiments reproduced the assemblage clinopyroxene + titanite ± K-feldspar (Fig. 1) via reactions of Ti-bearing biotite with quartz and plagioclase, initiated by the alkali-rich fluid. Under the run temperature, the assemblage clinopyroxene + titanite coexists with the melt of syenite composition enriched in volatiles (F, Cl and H_2O) (Table 1), which was confirmed using Raman spectroscopy. This is consistent with the proposed model for the syenite formation. Amphibole-bearing assemblages were produced in the experiments with high contents of NaCl in the fluid.

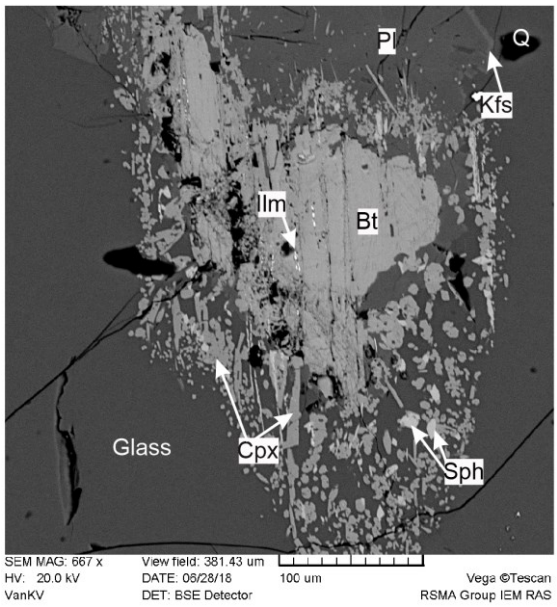

Fig. 1. Formation of the clinopyroxene (Cpx) + titanite (Sph) ± K-feldspar (Kfs) associated with the melt due to reactions of biotite, quartz and plagioclase.

Table 1. Average compositions of glasses in the run products.

Sample	SiO_2	Al_2O_3	CaO	Na_2O	K_2O	H_2O	Cl	F
1	70.55	12.07	0.90	2.67	6.26	1.57	0.04	0.11
3	64.96	15.87	1.56	3.79	4.85	4.27	0.04	0.25
4	61.08	20.69	2.63	5.79	5.47	2.94	0.03	0.03
5	68.15	12.23	0.92	4.59	3.35	1.87	0.34	0.26
6	62.20	15.50	1.25	3.95	4.81	2.36	0.04	bdl
7	66.93	15.46	0.70	2.86	7.11	3.95	0.04	0.26
8	67.10	12.78	0.65	2.67	5.37	2.82	bdl	bdl

Thus, the rocks of the Madiapala massif are a product of the syenitization of tonalite gneisses, which is in essence similar to granitization. Syenites of the Madiapala massif were formed at 6-9 kbar and 800-850°C via the active interaction of the Alldays TTG gneisses with an aqueous-carbonic-salt potassic fluids. The determining factor for the formation of the syenite assemblage was the increased potassium

activity in the fluid. Later amphibole-bearing assemblages were formed in the course of the syenite magma cooling. This stage corresponded to a change in the regime of alkaline components in fluid, so that the increase in Na_2O activity led to the replacement of the clinopyroxene + K-feldspar assemblage with the amphibole + albite assemblage.

The study was performed under the financial support of the Russian Science Foundation (project No. 18-17-00206) and partially under the Research Program AAAA-A18-118020590148-3 of the Korzhinskii Institute of Experimental Mineralogy RAS.

References

Connolly J. A. D. Computation of phase equilibria by linear programming: a tool for geodynamic modeling and its application to subduction zone decarbonation //Earth and Planetary Science Letters. – 2005. – T. 236. – №. 1-2. – C. 524-541.

Rigby M., Mouri H., Brandl G. PT conditions and the origin of quartzo-feldspathic veins in metasyenites from the Central Zone of the Limpopo Belt, South Africa //South African Journal of Geology. – 2008. – T. 111. – №. 2-3. – C. 313-332.

Rigby M. J., Armstrong R. A. SHRIMP dating of titanite from metasyenites in the Central Zone of the Limpopo Belt, South Africa //Journal of African Earth Sciences. – 2011. – T. 59. – №. 1. – C. 149-154.

Safonov O. G. et al. Experimental and petrological constraints on local-scale interaction of biotite-amphibole gneiss with H2O-CO2-(K, Na) Cl fluids at middle-crustal conditions: Example from the Limpopo Complex, South Africa //Geoscience Frontiers. – 2012. – T. 3. – №. 6. – C. 829-841.

Safonov O. G., Aranovich L. Y. Alkali control of high-grade metamorphism and granitization //Geoscience Frontiers. – 2014. – T. 5. – №. 5. – C. 711-727.

Safonov O. G., Kosova S. A., Van Reenen D. D. Interaction of Biotite–Amphibole Gneiss with H2O–CO2–(K, Na) Cl Fluids at 550 MPa and 750 and 800° C: Experimental Study and Applications to Dehydration and Partial Melting in the Middle Crust //Journal of Petrology. – 2014. – T. 55. – №. 12. – C. 2419-2456.

Shchekina T.I.[1], Zinovieva N.G.[1], Rusak A.A.[2], Khvostikov V.A.[3], Gramenitskiy E.N.[1], Alferyeva Ya.O.[1], Kotelnikov A.R.[4] Particularities of scandium distribution between silicate and salt melts and crystal phases in the Si-Al-Na-K-Li-F-O-H system AT 800°-500°C and 1 kbar.

UDC 552.11, 550.42

[1]Lomonosov Moscow State University, Department of Geology, Moscow, [2](GEOKHI RAS), Moscow, [3](IPTM RAS), [4](IEM RAS), Chernogolovka (t-shchekina@mail.ru; aleks7975@yandex.ru)

Abstract. The distribution of Sc in the Si-Al-Na-KFOH model granite system between aluminosilicate and LiKNa-aluminofluoride (salt) melts is studied at temperatures 800°-600°C and pressure 1 kbar .. It is shown that in the range of 800° - 700°C scandium accumulates along with rare-earth elements in salt melt with high distribution ratios >> 1. With a further decrease in temperature to 500 ° C, along with silicate (supercooled) and salt melts, crystalline phases are formed in the system - quartz, K-Na – aluminofluorides of the cryolite-elpasolite series and Li-containing polylithionite. It was found that scandium is included not only in the composition of silicate and salt melts, but also in aluminofluorides and mica. The Sc partition coefficient between aluminofluoride and silicate melt is about 5-15, between Na-aluminofluorides and the melt about 0.5; Na-K aluminofluorides - close to 5; between REE fluorides and silicate melt - 1-2, between mica and melt - 20. The highest partition coefficients of about 40 are observed between potassium and scandium rich fluoride and silicate melt. In all the mentioned crystalline phases of scandium, aluminum is apparently isomorphically replaced. This feature of scandium sharply distinguishes it from rare-earth elements and yttrium, which practically do not form part of cryolite-like phases and mica, and in the system under study only form their own fluoride phases of the LnF3 type, sometimes containing alkaline elements.

Keywords: *distribution, partition, rare-earth elements, scandium, lithium, silicate and aluminofluoride salt melts*

In previous works (Gramenitsky et al., 2005; Shchekina et al., 2013), it was shown that in a granite system with limiting fluorine contents at temperatures of 700-800 ° C, two immiscible melts are formed - silicate and salt (alkaline aluminum fluoride). The aim of the work was to establish the conditions and order of crystallization of these melts and the distribution of rare-earth elements, yttrium and scandium between the phases formed when the temperature of the system decreases from liquidus to solidus (from 800 to 500 ° C) at a pressure of 1 kbar. Previously, it was also found that in the range of 800 ° C - 700 ° C, scandium, along with rare-earth elements, accumulates in a salt melt with high separation coefficients >> 1. At lower temperatures, the distribution of these elements has not been studied. Compared to REE and Y, the behavior of Sc is characterized by a number of features (Shchekina and Gramenitsky, 2008; Shchekina et al., 2003), which are considered in this paper.

Technique and experimental technique. Analytical methods. *Source materials.* A silicate-salt mixture of reagents corresponding to composition A-40/11 was used as the initial charge. It was a composition of the aluminosilicate melt in the granite eutectic region, saturated with water and containing 1% F. The aluminofluoride component was added to this silicate composition (stoichiometric corresponding to the compound (Na, K, Li) 3AlF6 in an amount sufficient to saturate the aluminosilicate melt and appearance of the isolate aluminofluoride phase (Table. 1).

For the article, those experiments were selected in which the water content in the system was about 10 wt.%. The following reagents and compounds

were used as starting materials for the preparation of the mixture: dried gel SiO_2, NaF, LiF, AlF_3, Al_2O_3, K_2SiF_6. The rare-earth elements La, Ce, Pr, Nd, Sm, Eu, Gd, Tb, Dy, Ho, Er, Tm, Yb, Lu, and also Y and Sc were introduced into the system in the form of oxides in an amount of 0.5–2 wt%.

Table 1. The initial composition of the silicate-salt mixture (100%) - reference composition A-40/11 for all series of experiments (at.%).

Si	Al	Na	K	Li	F	O	Sum
17,24	6,92	5,07	3,84	4,46	21,82	40,65	100

Equipment and experimental techniques. The experiments were carried out on a high gas pressure unit with internal heating at a temperature of 500-800 ° C and a pressure of 1 kbar. The temperature measurement error was ± 5 ° C, pressure ± 10 bar. The volatility of oxygen in the experiments corresponded to that one created by the NNO + 3.5 buffer. The duration of the experiments was 7 days. Platinum ampoules with a diameter of 3 mm and a wall thickness of 0.2 mm were used as containers for the substance of the experiments. The experiments were carried out as follows. In experiments at 500-600 ° C, the approach to equilibrium "from above" was used. Ampoules with the substance were heated to 800 ° C and a pressure of 1 kbar, held for 3 days and then slowly cooled to a predetermined temperature for 8 hours. Then they were kept for 3 days at 600, 550 or 500 °C and quenched. The hardening rate at the installation was 150-200 degrees per minute.

Methods of electron microscopy and microprobe analysis. The structure of samples, the morphology of phases, phase relationships, and the chemical composition of the solid products of the experiments were studied at the Laboratory of Local Methods of Research of Substances of the Department of Petrology, Geological Faculty of Moscow State University. Electronic images are obtained in reflected electron mode (BSE). The analysis of the main elements and fluorine in phases was carried out using a Jeol JSM-6480LV scanning electron microscope (Japan) with an energy-dispersive Oxford X-MaxN and INCA Wave-500 crystal diffraction spectroscopes (Oxford Instrument Ltd., UK). Shooting conditions: voltage 20 kV, current 0.7 nA. The accuracy of the estimation of the main elements in the composition of the synthesized phases was 2–5 rel.%. The instrumental error in the measurement of fluorine was ± 1% of the element concentration.

In a number of samples, the main and rare-earth elements in silicate glasses were studied using a Superprobe JXA-8230 electron probe microanalyzer (Japan). To prevent glass destruction, the analyzes were performed in the defocused beam mode (up to 10 μm) at an accelerating voltage of 10 kV and a current strength of 10 nA. At the time of measuring the peak and background intensities (30/15 sec), the dispersion of the measurements of Si, Al, and O was 0.8 rel.%, K was 1.5 rel.%, Na was 2 rel.%, And F was 2 rel. % Rare earth elements were analyzed at an accelerating voltage of 20 kV and a current of 30 nA. The accumulation time for various rare-earth elements was selected so that their detection limit did not exceed 0.01%.

Inductively coupled plasma mass spectrometry and laser ablation. Inductively coupled plasma mass spectrometry and laser ablation. The rare-earth elements, Li, Sc, and Y were also determined in aluminosilicate glass and in the salt phase in polished samples by inductively coupled plasma mass spectrometry and laser ablation at the Analytical Certification Test Center of the Institute for Problems of Microelectronics and Particular Materials Technology of the Russian Academy of Sciences (ASIC IPTM RAS) . The measurements were performed on an inductively coupled plasma quadrupole mass spectrometer X Series II (Thermo Scientific, USA) with an UP266 MACRO laser ablation attachment (New Wave Research, USA). Conditions for its operation: laser wavelength 266 nm, pulse repetition rate 10 Hz, pulse energy 3 mJ, pulse duration 4 ns, crater diameter 60 μm. The time of one measurement was 10 s. External calibration was performed using standard samples of NIST SRM-610 ¬ ÷ 616 silicate glass. Silicon was used as the internal standard. In addition, an additional correction of the matrix was carried out, taking into account that the elements of the glass phase base are in the form of oxides in it and the salt phase in the form of fluorides. The limits for the determination of elements found using the 3σ criterion (with a confidence probability of P = 0.95) for REEs range from 1 × 10-7 to 1 × 10-6 mass%; the relatively high limit for Sc 2 × 10–4 wt.% is due to polyatomic interference: ^{45}Sc ($28Si_{17}OH$, $^{29}Si_{16}O$).

The results of the experiments. The phase composition of the material of experiments carried out at 800, 750, and 700 ° C is represented by glass-tempered aluminosilicate melt (L) and salt melt (LF), represented by globules that crystallized during quenching and are folded by an alkaline aluminofluoride aggregate (Na, K, and Li) and rare earth, yttrium and scandium fluorides, (Table 2). In the range of 800 -700 ° C, no crystalline phases form in the glass. In large globules of the salt phase at 700 ° C, KNa aluminofluoride (FP1) begins to crystallize, similar in cryolite stoichiometry. It forms crystals of isometric, often rounded, cross-sectional size from 20 to 100 μm (Fig. 1a, b), which occupy more than 1/2 of the globule volume.

Table 2. Average aluminosilicate (L) and salt (LF) melts and compositions of fluoride crystalline phases (FP) in experiments conducted at 500-800 ° C and 1 kbar (wt.%).

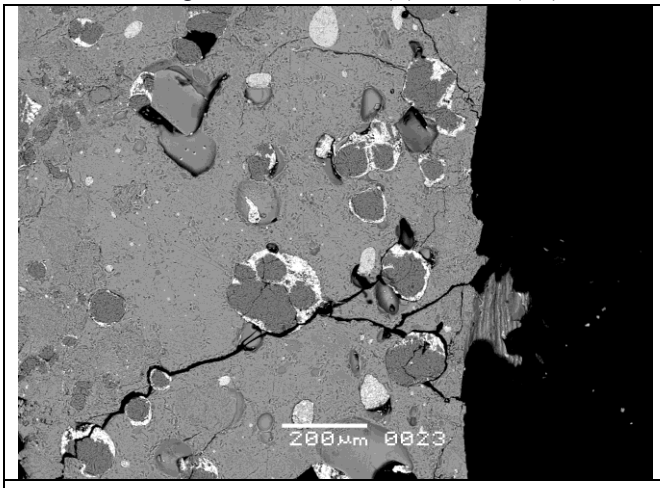

Fig. 1.a. Globules of molten salt (600 ° C) immersed in aluminosilicate glass.

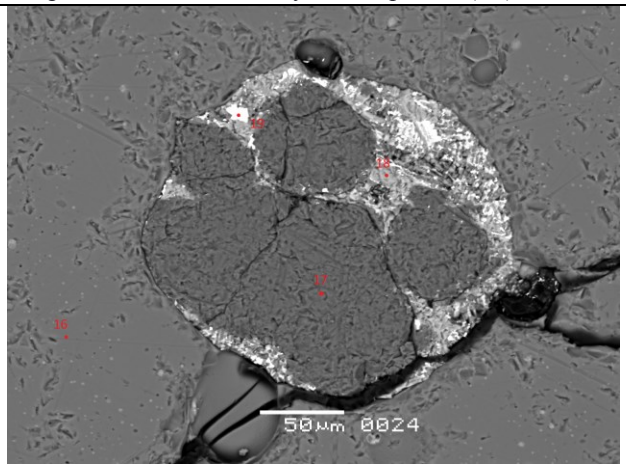

Fig. 1b. Crystals of Na aluminum fluoride (dark gray in BSE) and residual salt melt (light gray in BSE), rich in REE, Sc, Y within the boundaries of the salt globule.

Notes to the Table. The composition was determined: 1 - the main elements using the INCA Wave-500 microprobe (Oxford Instrument Ltd., REE, Sc - laser ablation; 2 - using the INCA Wave-500 microprobe (Oxford Instrument Lt .; 3 - using the electron Superprobe JXA-8230 Probe Microanalyzer. 4 — Presumably, polylithionite The Li content was estimated by the difference in the sum of the analysis.

T°C, №.	Phases	Si	Al	Na	K	Mg	Ca	Li	F	O	Sc	∑REE	Sum
	Start comp.	19,99	7,73	4,83	6,20	n.d.	n.d.	1,30	17,16	35,86	**0,42**	6,52	100,0
800°C 777[1]	L(4)	26,45	7,27	3,06	7,22	n.d.	n.d.	0,47	17,27	38,16	**0,01**	0,08	100,0
	LF(4)	0,65	8,89	16,97	6,34	n.d.	n.d.	4,87	55,53	3,12	**0,21**	3,42	100,0
	Kp(LF/L)	0,02	1,22	5,55	0,88	n.d.	n.d.	10,25	3,22	0,08	**17,19**	41,61	
700°C 820[1]	L (3)	27,80	7,73	2,41	7,45	n.d.	n.d.	0,41	9,27	43,65	**0,06**	1,21	100,0
	LF (3)	0,32	9,43	15,72	6,32	n.d.	n.d.	1,25	55,79	3,25	**0,30**	7,63	100,0
	Kd (LF/L)	0,01	1,22	6,51	0,85	n.d.	n.d.	3,04	6,02	0,07	**4,63**	6,30	
600°C 871[2]	L (3)	28,09	7,39	2,19	7,32	0,00	0,00	n.d.	9,55	44,45	0,49	0,53	100,0
	LF (2)	0,22	3,07	9,77	4,77	0,33	0,51	n.d.	49,06	3,57	13,10	15,61	100,0
	Kd LF/L	0,01	0,42	4,46	0,65	n.d.	n.d.	n.d.	5,14	0,08	26,78	59,36	
	FP1 (2)	0,04	13,46	22,42	2,04	0,00	0,06	n.d.	60,87	0,38	0,47	0,25	100,0
	Kd(FP1/L)	0,00	1,82	10,23	0,28	n.d.	n.o.	n.d.	6,38	0,01	0,96	0,72	
	FP 3 Sc (2)	0,00	0,00	0,32	11,15	0,33	0,12	n.d.	38,99	1,30	19,39	28,41	100,0
	Kd(FP3/L)	0,00	0,00	0,15	1,52	n.d.	n.d.	n.d.	4,08	0,03	39,64	83,88	
	FP4REE(2)	0,00	0,00	3,72	1,45	0,00	1,20	n.d.	28,94	0,38	1,14	63,18	100,0
	Kd(FP4/L)	0,00	0,00	1,70	0,20	n.d.	n.d.	n.d.	3,03	0,01	2,33	119,2	
500°C 890[3]	L(7)	31,77	7,22	1,52	6,03	0,00	0,01	0,79	5,80	46,86	0,09	0,01	100,10
	FP1 (9)	0,02	14,14	24,18	3,42	0,02	0,07	1,63	56,23	n.d.	0,34	0,04	100,1
	Kd (FP1/L)	0,00	1,96	15,88	0,57	3,61	10,30	2,08	9,70	n.d.	3,89	3,78	
	FP2 (8)	0,10	6,95	9,23	29,85	0,01	0,04	2,84	45,41	n.d.	5,58	0,04	100,0
	Kd (FP2/L)	0,00	0,96	6,06	4,95	1,34	6,81	3,61	7,83	n.d.	63,80	3,76	
	Pol^{4-} (4)	27,23	6,22	0,05	10,04	0,02	0,04	4,87	9,05	40,68	1,80	0,02	100,0
	Kd (Pol/L)	0,86	0,86	0,03	1,66	3,76	5,63	6,19	1,56	0,87	20,59	1,40	
At.%	Pol (4)	18,57	4,41	0,04	4,92	0,01	0,02	13,42	9,12	48,71	0,77	0,00	100,0

They are homogeneous in composition with a significant predominance of Na over K (Table 2, FP 1). They have a small Sc content (about 1 wt.%). The rest of the globule space is occupied by a melt (LF), which surrounds the crystals, penetrates between them and is located along the boundary with silicate glass. Apparently, this residual melt was rather mobile (Fig. 1b). It consists of numerous quenching fluoride phases of rare earth elements in association with alkali fluorides –Na, K, and Li. As the temperature decreases from 700 to 500 ° C, alkali aluminum fluoride crystals occupy ever larger

volume within the salt globules (Fig. 1 a, b). Starting from 600 ° C, similar phases (FP2) are added to essentially sodium aluminofluorides, but with a high K content (K >> Na). They are usually enriched in Sc (FP2). In addition, fluoride phases appear in which Na and K are contained, and the main trivalent cation is Sc (FP3) (Table 2, FP3), which acts as Al. This phase contains about 5 wt.% Sc. Rare earth elements and yttrium form, as a rule, fluorides of the LnF3 type or alkaline rare earth fluorides (FP4) (Table 2). In these phases, Sc contains only about 1%. REE phases up to 500 ° C remain within the volume of globules in association in alkali fluorides, crystallizing with them from the residual salt melt last. It increases the number of rare-earth phases, as can be judged by electronic photographs, namely, the abundance of light emissions of REE fluorides of various shapes. The separation coefficients Sc between the above phases (LF, FP) and L can be seen in theTtable. 2. For Sc, they are always higher than 1, that is, Sc is distributed in favor of certain fluoride phases in comparison with silicate melt.

When the temperature decreases below 700 ° C, quartz and 2 types of aluminofluorides enriched in Na (FP1) and rich in K (FP2) crystallize in aluminosilicate glass. They crystallize in the form of round or idiomorphic crystals with a cross-sectional size of up to 20 microns. Sometimes they are observed inside large quartz grains, which indicates their simultaneous crystallization. Such relationships of quartz with cryolite are found in cryolite-containing granites.

It has been found that scandium is contained in almost all fluorine-containing phases crystallizing in the system, with the ability to adapt to the structures of various minerals. It is included not only in the composition of silicate and, especially, salt melts, but also in aluminofluorides and mica. The partition coefficient Sc between aluminofluoride and silicate melt is about 5-15, between Na-aluminofluorides and melt about 0.5; Na-K aluminofluorides - close to 5; between REE fluorides and silicate melt - 1-2, between mica and melt - 20. The highest separation coefficients of about 40 are observed between potassium rich and scandium fluoride and silicate melt. In the crystalline phases mentioned, aluminum is apparently isomorphically replaced by scandium. This feature of scandium sharply distinguishes it from rare-earth elements and yttrium, which practically do not form part of cryolite-like phases and mica, and in the system under study only form their own fluoride phases of the LnF3 type or fluorides containing alkaline elements of the gagarinite type.

This work was financially supported by the RFBR grant No. 16-05-0089.

References

Gramenitsky E.N., Schekina T.I., Devyatova V.N. (2005) Phase relations in fluorine-containing granite and nepheline-syenite systems and distribution of elements between phases. M .: GEOS. 186 p.

Schekina T.I., Gramenitsky E.N., Alfer'eva Y.O. (2013). Leucocratic magmatic melts with limiting fluorine concentrations: experiment and natural relationships. Petrology 21 (5), 499-516.

Suk N.I., Kotelnikov A.R., Viryus A.A Experimental studies of loparite solubility in silicate melts

Institute of Experimental Mineralogy RAS (IEM RAS), 142432, Chernogolovka, Moscow district, Russia (sukni@iem.ac.ru; kotelnik@iem.ac.ru)

Abstract. The solubility of loparite in aluminosilicate melts of various compositions was experimentally studied at T=1200 and 1000°C and P=2 kbar in dry conditions and in the presence of 10 wt.% H_2O. The experiments were carried out on a high gas pressure vessel. The duration of the experiments was 1 day. The starting material was synthetic glass of malignite, urtite, and eutectic albite-nepheline composition, previously melted at T=1450°C in a furnace with chromite-lanthanum heaters in platinum crucibles for 2 hours, as well as the natural loparite of the Lovozero massif. The composition of the samples after the experiments was determined by the method of electron probe x-ray spectral analysis. It was established that the solubility of loparite depends on the composition of the aluminosilicate melt (Ca/(Na + K), (Na + K)/Al). The partition coefficients of a number of elements between the silicate melt and loparite crystals ($K_i = C_i^{melt}/C_i^{lop}$) are estimated.

Keywords: silicate melt, loparite, solubility, experiment

The solubility of loparite in aluminosilicate melts of various compositions was experimentally studied at T=1200 and 1000°C and P=2 kbar under dry conditions and in the presence of 10 wt% H_2O. The experiments were carried out on a high gas pressure vessel. The duration of the experiments was 1 day. The starting material was synthetic glasses of malignite, urtite and eutectic albite-nepheline composition, preliminarily melted at T=1450°C in a furnace with chromite-lanthanum heaters in platinum crucibles for 2 hours, as well as natural loparite from the Lovozero massif. The compositions of the samples after the experiments were determined on a Tescan Vega II XMU scanning electron microscope (Czech Republic) equipped with energy dispersive (INCAx-sight) and crystal diffraction (INCA wave) X-ray spectrometers (England, Oxford). The program of qualitative and quantitative analysis INCA Energy 450 was used. The analysis of the samples was carried out using both energy dispersive (for the main rock-forming elements) and crystal-diffraction (for Sr, Nb, La, Ce, Nd) spectrometers.

During the experiments, the aluminosilicate melt was saturated with elements characteristic of loparite. In this case, in the malignite melt, the formation of rims on loparite crystals differing in composition from loparite was observed (Fig. 1). In the rims, the contents of Na_2O, SrO, Nb_2O_5 decrease, and to a lesser extent TiO_2. Due to this, the relative contents of rare earth elements increase. This indicates that Ti, Na, Sr, and Nb migrate from loparite to alkaline melt more easily than REE. In aqueous systems, the border is more pronounced than in dry systems. This is also evidenced by estimates of the partition coefficients of elements between loparite crystals and melt (C_i^{melt}/ C_i^{lop}, where C is the concentration of oxides in wt %). In the melt of malignite and albite-nepheline composition at T=1000°C and P=2 kbar, the average values of the partition coefficients for TiO_2 and SrO are practically the same: 0.065 and 0.311 (in the melt of malignite composition) and 0.065 and 0.316 (in the melt of albite-nepheline composition), respectively. For Nb_2O_5, La_2O_3, Ce_2O_3, and Nd_2O_3, the average partition coefficients are much lower in experiments with a melt corresponding to the composition of the albite-nepheline eutectic: K_{Nb2O5}=0.037 (0.079), K_{La2O3}=0.023 (0.044), K_{Ce2O3}=0.022(0.042), K_{Nd2O3}=0.021(0.052). Values for experiments with melt of malignite composition are given in brackets. At T=1200°C and P=2 kbar, a similar pattern is observed. The average values of the partition coefficients decrease in melts corresponding to the composition of the albite-nepheline eutectic: K_{TiO2}=0.068(0.097), K_{SrO}=0.107(0.116) K_{Nb2O5}=0.050(0.086), K_{La2O3}=0.005(0.013), K_{Ce2O3}=0.021(0.048), K_{Nd2O3}=0.015(0.040). Values for experiments with melt of malignite composition are given in brackets.

In the melt, corresponding to the composition of the albite-nepheline eutectic, the formation of crystals of rare-earth titanosilicates was observed (Fig. 2), and in water-containing systems, sometimes rare earth titanoniobates growing on loparite crystals were also observed.

Apparently, the formation of such crystals, as well as the rims around loparite grains, may indicate that the incongruent dissolution of loparite in melts takes place.

The solubility of loparite can be estimated by determining the sum of rare earth oxides (La_2O_3, Ce_2O_3, Nd_2O_3) and oxides of elements inherent only to loparite (TiO_2, Nb_2O_5, SrO) in the glass obtained as a result of the experiment. The presence of water had practically no effect on the solubility of loparite. It was found that the solubility of loparite depends on the composition of the aluminosilicate melt (Fig. 3): it increases with an increase in the agpaitic coefficient of the melt ((Na+K)/Al) and with an increase in the Ca/(Na+K) ratio. According to the estimates, the solubility of loparite in a melt of malignite composition at T=1000°C and P=2 kbar is on average ~ 6 wt%, in a melt corresponding to the composition of an albite-nepheline eutectic – on average ~ 5.2 wt%, and in a melt corresponding to the composition of urtite ~ 3.7 wt%, and at T=1200°C and P = 2 kbar in the melt of malignite composition ~ 6.34 wt% and in the melt corresponding to the composition of the albite-nepheline eutectic ~ 4.35 wt%.

Such solubility values are insufficient to explain the loparite content in the malignite horizon, to which the rich loparite ores of the Lovozero alkaline massif are confined. The content of loparite in malignite reaches 20-25%. The data obtained can explain the presence of accessory loparite in the rocks.

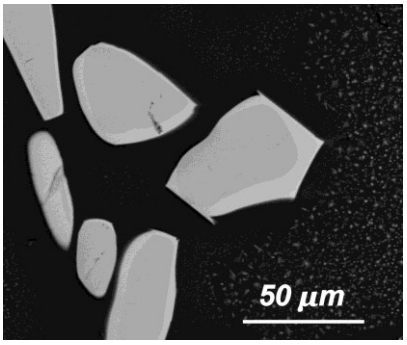

Fig. 1. Borders formed on loparite crystals in experiments with malignite melt at T=1200°C and P=2 kbar.

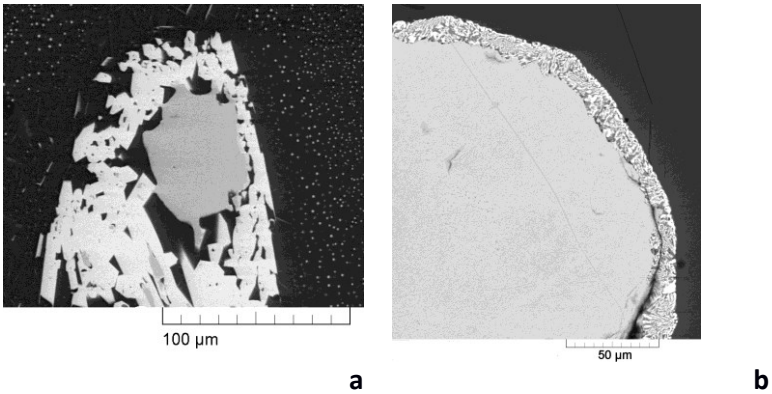

Fig. 2. Formation of rare earth titanosilicate crystals around loparite grains in a melt corresponding to the composition of the albite-nepheline eutectic at T=1200°C and P=2 kbar.

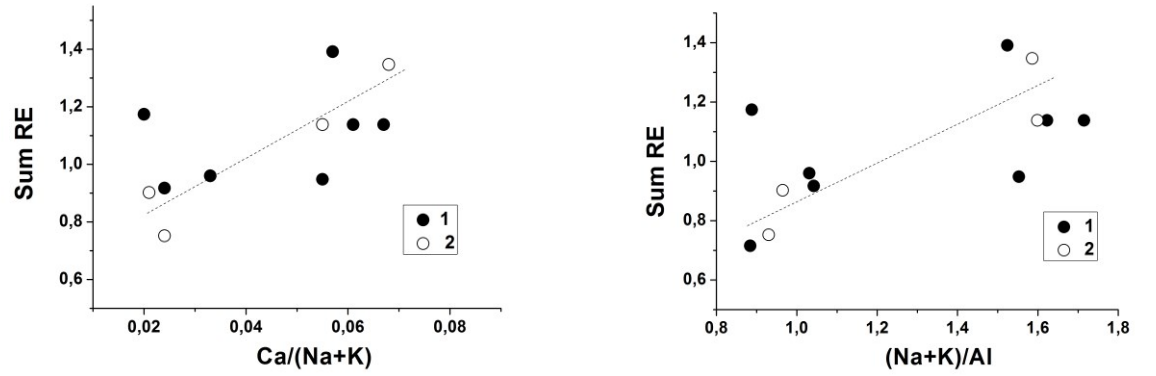

a **b**

Fig. 3. Dependence of the solubility of loparite on Ca/(Na+K) of the aluminosilicate melt (a) and on the agpaitic coefficient ((Na+K)/Al) of the aluminosilicate melt (b). Sum RE=Ti+Nb+Sr+La+Ce+Nd, form. units 1 – T=1000°C, 2 kbar; 2 – T=1200°C, 2 kbar. Form. units – formula units obtained by recalculating the analysis of silicate melt per 50 oxygen atoms.

In water-containing systems, the formation of an emulsion was constantly observed, expressed in the presence of small droplets enriched with elements characteristic of loparite. Apparently, this is a manifestation of titanate-silicate liquid immiscibility, which was obtained earlier (Suk, 2007, 2012) in water-bearing aluminosilicate systems containing ore elements (Ti, Nb, Sr, REE). The presence of the emulsion made it difficult to analyze the glasses, the compositions of which were determined in the purest regions of the melt.

Thus, the experimental data obtained show that rich loparite ores cannot be formed by direct crystallization of loparite from the melt. Their formation can only be explained by the occurrence of titanate-silicate immiscibility, as a result of which the magmatic melt is significantly enriched in ore components.

This work was supported by the AAAA-A18-118020590151-3 program.

References

Suk N.I. Experimental study of alkaline magmatic aluminosilicate systems: implication for the genesis of REE-Nb loparite deposits. Doklady Earth Sciences. 2007. V. 414. No 1. P. 615-618.

Suk N.I. Experimental study of liquid immiscibility in the fluid-magmatic silicate systems containing Ti, Nb, Sr, REE, and Zr. Petrology. 2012. V. 20. N 2. P.138-146.